

Boundary quantum phase transitions in the spin- $\frac{1}{2}$ Heisenberg chain with boundary magnetic fields

Parameshwar R. Pasnoori ^{1,2,*}, Junhyun Lee ^{3,*}, J. H. Pixley ^{3,4}, Natan Andrei ³ and Patrick Azaria⁵

¹*Department of Physics, University of Maryland, College Park, Maryland 20742, USA*

²*Laboratory for Physical Sciences, 8050 Greenmead Dr, College Park, Maryland 20740, USA*

³*Department of Physics and Astronomy, Center for Materials Theory, Rutgers University, Piscataway, New Jersey 08854-8019, USA*

⁴*Center for Computational Quantum Physics, Flatiron Institute, New York, New York 10010, USA*

⁵*Laboratoire de Physique Théorique de la Matière Condensée, Sorbonne Université and CNRS, 4 Place Jussieu, 75252 Paris, France*



(Received 13 February 2023; revised 17 April 2023; accepted 2 June 2023; published 12 June 2023)

We consider the spin-1/2 Heisenberg chain with boundary magnetic fields and analyze it using a combination of Bethe ansatz and density matrix renormalization group (DMRG) techniques. We show that the system exhibits several different ground states, which depend on the orientation of the boundary magnetic fields. When both the boundary fields take equal values greater than a critical field strength, each edge in the ground state accumulates a fractional spin which saturates to spin 1/4, which is similar to systems exhibiting symmetry protected topological phases (SPT). Unlike in SPT systems, the fractional boundary spin in the Heisenberg spin chain is not a genuine quantum number since the variance of the associated operator does not vanish, this is due to the absence of a bulk gap. The system exhibits high-energy bound states when the boundary fields take values greater than the critical field. All the excitations in the system can be sorted out into towers whose number depends on the number of bound states exhibited by the system. As the boundary fields are varied, in addition to the ground-state phase transition, we find that the system may undergo a boundary eigenstate phase transition (BEPT) where the number of towers of the Hilbert space changes. We further inquire how the EPT reflects itself on local ground-state properties by computing the magnetization profile $\langle S_j^z \rangle$ using DMRG. We identify a clear qualitative change from low edge fields to high edge fields when crossing the critical field. We though are unable to conclude on the basis of our data that EPT corresponds to a genuine phase transition in the ground state.

DOI: [10.1103/PhysRevB.107.224412](https://doi.org/10.1103/PhysRevB.107.224412)

I. INTRODUCTION

The Heisenberg model is one of the most celebrated models in condensed matter and statistical physics. It lies at the cornerstone of our understanding of many physical phenomenon which, besides magnetism, consists of integrability [1–3], many body localization [4,5], and out of equilibrium dynamics [6–8]. Thanks to available analytic and numerical methods the model is quite well understood in one spatial dimension. This is partly due to the fact that the one dimensional spin $S = 1/2$ Heisenberg model, which is also known as the XXX spin chain, is integrable. At the same time, the model can be probed experimentally either in solid-state compounds comprising quasi-one-dimensional spin chains in KCuF_3 [9–13] or more recently in ultracold atom realizations of the spinful Bose-Hubbard model [14,15]. Since it was first solved by Bethe [1], the spin chain with periodic boundary conditions has been very well studied. Both the ground-state and the low-energy excitations properties are well understood [3,16–19]. The system is nonmagnetic and supports massless spin-1/2 excitations named spinons. Besides this, integral representations of correlation functions have been obtained

[20–22]. Spin chains with open boundaries have also been intensely studied after the Yang-Baxter algebra was generalized to systems with open boundaries by Sklyannin and Cherednik [2,23]. For the XXX spin chain with open boundaries the ground state, bulk excitations and physical boundary S matrices have been found [24]. More generally the effects of boundary fields [25–27] have also been investigated and spin chains with nondiagonal boundary fields have been solved [28].

In this work, we shall be interested in the XXX spin chain with magnetic fields at its edges. Although the subject has been studied to some extent, for a quantum impurity [29] as well as for a classical one (e.g., with boundary magnetic fields), we find that some issues remain to be clarified and explored in the light of new developments related with one dimensional topological phases and eigenstate phase transitions. To the best of our knowledge, the results that will be presented in this work have not been found before.

The Hamiltonian of the XXX spin chain with boundary magnetic fields is given by

$$H = \sum_{j=1}^{N-1} \sum_{\alpha=x,y,z} \sigma_j^\alpha \cdot \sigma_{j+1}^\alpha + h_L \sigma_1^z + h_R \sigma_N^z, \quad (1)$$

where σ_j^α are the Pauli matrices acting on the spin space at site j , h_L and h_R are boundary magnetic fields acting at sites

*These authors contributed equally to this work.

†pparmesh@umd.edu

‡junhyun.lee@physics.rutgers.edu

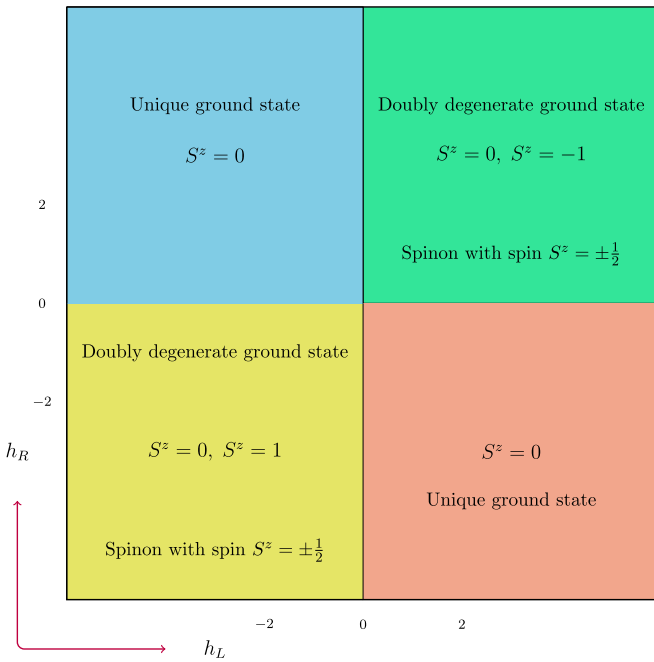


FIG. 1. Various ground states occurring for different values of the boundary magnetic fields for an even number of sites chain in the thermodynamic limit [34]. The ground state is unique in the second and fourth quadrants. In the first and third quadrants, the ground state contains a spinon with infinite rapidity and whose spin is oriented either in the positive or negative z direction, resulting in a twofold degenerate ground state.

$j = 1$ and $j = N$, respectively, and N is the number of sites. The boundary magnetic fields break the $SU(2)$ spin symmetry down to the $U(1)$ group of rotation around the z axis. There exists no other symmetries except when $h_L = h_R$, where the model displays space parity invariance \mathbb{P} . Despite this, the system possesses a useful isometry obtained by simultaneously flipping all spins as well as reversing the orientation of the boundary fields:

$$H \rightarrow \prod_{i=1}^N \sigma_i^x H \sigma_i^x, \quad h_L \rightarrow -h_L, \quad h_R \rightarrow -h_R. \quad (2)$$

The latter isometry is a symmetry of the phase diagram of the model in the plane (h_L, h_R) . The Hamiltonian (1) is integrable by the method of the Algebraic Bethe Ansatz. The Bethe equations associated with the Hamiltonian (1) and spin-1/2 XXZ chain with boundary fields have been first obtained in Ref. [30] for special values of the boundary fields using the method of coordinate Bethe ansatz, and were later obtained in Ref. [2] using algebraic Bethe ansatz for general diagonal boundary fields and were analyzed in Refs. [24,31–33]. In the present work, we shall extend their analysis and present a more thorough picture of the phase diagram associated with (1), thus providing important new results that have not been, to the best of our knowledge, present in the literature. However, before going into more details let us first discuss qualitatively our main results.

We first discuss the ground-state properties of the model. We present in Fig. 1 the ground-state phase diagram in the

plane (h_L, h_R) and for an even number of sites. A similar analysis can be made for an odd number of sites as given in Sec. II. There are four different possible ground states when labeled by the conserved total z component of the spin operator,

$$S^z = \frac{1}{2} \sum_{j=1}^N \sigma_j^z. \quad (3)$$

When $h_L h_R < 0$ the ground state is unique and has total spin $S^z = 0$ whereas, contrarily to what was found in Ref. [32], in the quadrants $h_L h_R > 0$, we find that the ground state is doubly degenerated *in the thermodynamic limit* [34]; each one having spin $S^z = 0$ and $S^z = +1$ or $S^z = -1$ depending on whether $h_{L(R)}$ is negative or positive. In the later cases, the degeneracy is found to be the consequence of the existence of two static spinons (with infinite rapidity) with spins $\pm 1/2$ in the ground state. To get a better understanding of the ground-state structure, we have performed extensive density matrix renormalization group (DMRG) calculations and calculated the magnetization profile $\langle S_j^z \rangle$ in the ground state. Overall we find that the edge magnetic fields induce a spin polarization close to the two edges which extends into the bulk in a power-law fashion. Furthermore, we find that the corresponding spin accumulations at the edges are *fractional* and take the values $\pm 1/4$ (opposite to the orientation of the edge field) at large fields $|h| > 2$. The situation at hand is similar to what happens in gapless symmetry protected topological (SPT) superconductors [35–38] where the edge states Hilbert space is exhausted by spin-1/4 operators. However, in the present case, due to the existence of massless spinon bulk excitations, such an operator do not represent a genuine fractional sharp quantum observable since, as we show in Sec. IV, its variance is not zero.

The second topic we shall discuss in this work concerns the structure of the excited states and its relation to the existence of bound states localized at the edges. One of the hallmarks of the boundary physics induced by the edge magnetic fields is the existence of boundary bound states localized close to the edges where the fields are applied. As previously found in Refs. [31,32], when the magnitude of fields are large enough, i.e., when $|h_{L(R)}| \geq 2$, the system hosts bound states with energy

$$m_{L,R} = 2\pi / \sin\left(\frac{\pi}{h_{L,R}}\right), \quad (4)$$

which carry a spin-1/2, whose spin orientation is *along* the boundary fields at each edge. Contrarily to the zero energy edge states in SPT massless superconductors, the bound states in the XXX model are high-energy states whose energies are always above the one spinon branch of massless bulk excitations, and as we shall see, their existence has important consequences on the structure of the Hilbert space. We present in Fig. 2 the bound state phase diagram of the model (1). In each quadrant, the different phases are sorted out as a function of the number of bound states: the *A* subphases support two bound states (one at each edge), the *B* subphases support one bound state at either the right or the left edge, whereas in the *C* subphases there are no bound states. When compared to the ground-state phase diagram we see that each

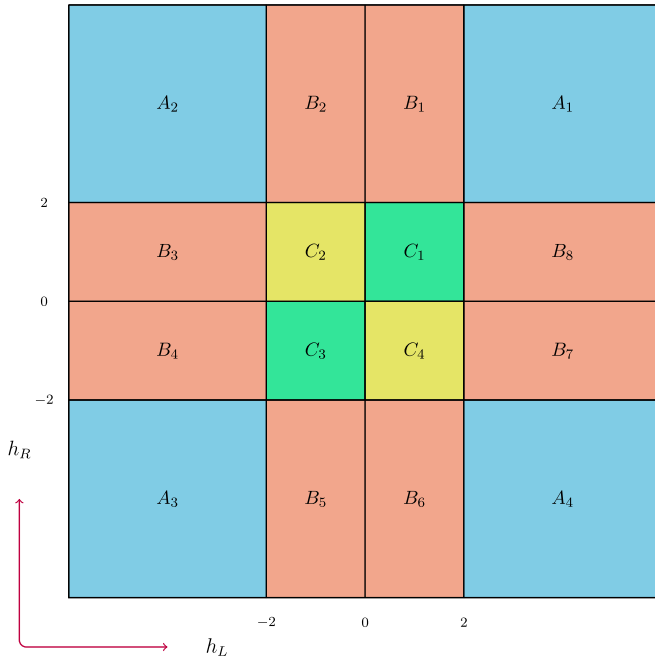


FIG. 2. Various phases occurring for different values of the boundary magnetic fields. The A subphases exhibit two boundary bound states, one at each edge. In B subphases, there exists one boundary bound state at either the left or the right edges. In C subphases, boundary bound states do not exist.

quadrant is split into three different subphases named A , B , or C . Although in all these subphases the ground state has the same total spin S^z , they differ by the structure of the high-energy states. We show that each bound state generates a whole tower of excited states that can be built upon it. Hence, the Hilbert space is comprised of a certain number of towers which depends on the number of bound states exhibited by the system. In [39], the author studied a more general spin $1/2$ -XYZ chain with open boundaries, which includes XXZ as a special case, where it was demonstrated that in the gapped regime of the XXZ chain the Hilbert space is comprised of two towers of degenerate eigenstates which leads to the emergence of a strong zero energy Majorana operator (which commutes with the Hamiltonian) which map these pairs of states.

In each of the A , B , and C subphases, the direct sum of these towers span the complete Hilbert space. When crossing the boundaries between any two of these subphases, since the number of bound states exhibited by the system and hence the number of towers of the excited states changes, a boundary eigenstate phase transition occurs which involves a full reorganization of the Hilbert space. A similar phenomenon is observed in gapless SPT superconductors [38].

In summary, we find that similar to the systems exhibiting SPT [38] the XXX spin chain exhibits several phases as a function of edge magnetic fields. We find that the total spin of the ground state is not enough to completely characterize these phases which differ also by the structure of the Hilbert space. The later is linked to the number of bound states at the edges which generate towers of excited states that together span the Hilbert space. As a consequence, on top of

the phase transition corresponding to a change in the ground state, there exists boundary eigenstate phase transitions involving the change in the number of towers of the Hilbert space.

The paper is organized as follows. We present our results obtained from the Bethe ansatz for the ground state and the excited states in Secs. II and III, respectively. Section IV is dedicated to the DMRG analysis of the ground-state properties. We finally discuss our results in Sec. V.

II. GROUND-STATE PHASE DIAGRAM

As said above, Hamiltonian (1) is integrable by the method of the algebraic Bethe ansatz [24,28] for arbitrary values of the boundary fields. Its ground state as well as excitations are obtained from the Bethe equations

$$\begin{aligned} & \left(\frac{\lambda_j - i/2}{\lambda_j + i/2} \right)^{2N} \left(\frac{\lambda_j + i(\frac{1}{2} - p_L)}{\lambda_j - i(\frac{1}{2} - p_L)} \right) \left(\frac{\lambda_j + i(\frac{1}{2} - p_R)}{\lambda_j - i(\frac{1}{2} - p_R)} \right) \\ &= \prod_{j \neq k=1}^{M-1} \left(\frac{\lambda_j - \lambda_k - i}{\lambda_j - \lambda_k + i} \right) \left(\frac{\lambda_j + \lambda_k - i}{\lambda_j + \lambda_k + i} \right), \end{aligned} \quad (5)$$

where we have introduced $p_{L/R} = 1/h_{L/R}$ as the boundary parameters. The eigenstates of the Hamiltonian are labeled by $M \in \mathbb{N}$ Bethe roots $\lambda_{j=1, \dots, M}$, which are solutions of Eq. (5) and have energy

$$E = - \sum_{j=1}^M \frac{2}{\lambda_j^2 + \frac{1}{4}} + N - 1 + h_L + h_R. \quad (6)$$

The corresponding total spin S^z of a state is related to the integer M through the relation (7)

$$S^z = \pm \left(\frac{N}{2} - M \right), \quad (7)$$

where \pm corresponds to reference state with all spin up and down, respectively. We have obtained from (5) the ground-state phase diagram as a function of the boundary magnetic fields $h_{L(R)}$ and for both an even and an odd number of sites. Before going into more details let us first review briefly the situation at zero fields. In this case, the ground state depends on the parity of N as follows. For even N , it is nondegenerated and has total spin $S^z = 0$ whereas for odd N it is twofold degenerated, each ground state having total spin $S^z = \pm 1/2$. The latter degeneracy is due to the presence of spin- $\pm 1/2$ spinons with rapidity θ , which have energy

$$E_\theta = \frac{2\pi}{\cosh(\pi\theta)} \quad (8)$$

and is zero in the limit of infinite rapidity $\theta \rightarrow \infty$. Notice that the above results have been rigorously proved using Perron-Frobenius theorem [40,41] in the case of zero edge fields. We are not aware of the extension of the above theorem to nonzero edge fields.. We will now show using Bethe ansatz how this scheme is modified in the presence of nonzero boundary fields. The situation further depends on the parity of N .

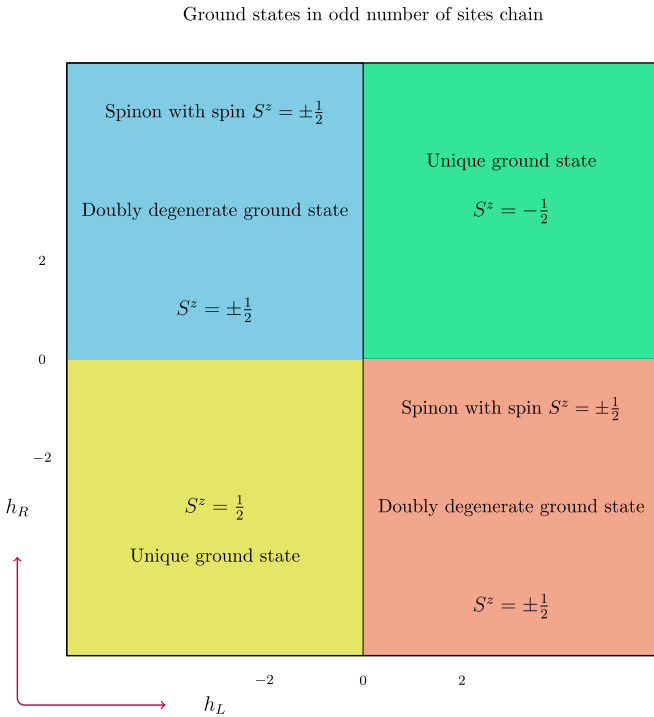


FIG. 3. Ground state phase diagram as a function of the boundary fields for an odd number of sites in the thermodynamic limit [34]. The ground state is unique in the first and third quadrants. In the second and fourth quadrants, the ground state contains a spinon with infinite rapidity and whose spin is oriented either in the positive or negative z direction, resulting in a twofold degenerate ground state.

A. Ground state for the odd number of sites

Since the total number of sites is odd the spins of the ground states have to be half integers. The phase diagram can be broadly divided into four quadrants based on the direction of the boundary magnetic fields as shown in the Fig. 3. In the upper right quadrant, when both the magnetic fields point towards the positive z direction, and independently of their magnitudes $|h_{L(R)}|$, the ground state is unique and has a total spin $S^z = -1/2$. In the ground state, which we shall label

$$\left| -\frac{1}{2} \right\rangle, \quad (9)$$

the total magnetization is due to a static spin configuration which account for the total spin $-1/2$. In the lower right quadrant, in which $h_L > 0$ and $h_R < 0$, the ground state is doubly degenerated [42] and carry total spins $S^z = \pm 1/2$

$$\left| -\frac{1}{2} \right\rangle \text{ and } \left| +\frac{1}{2} \right\rangle. \quad (10)$$

In contrast with the previous case, the spins of the ground states here is due to the presence of spin- $\pm 1/2$ spinons with infinite rapidity $\theta \rightarrow \infty$ (8). The situation in the two other quadrants, i.e., the lower left and upper left ones, can be obtained by using the isometry (2) and reversing the total spin quantum number $S^z \rightarrow -S^z$. The ground states are then found to be

$$\left| +\frac{1}{2} \right\rangle \text{ and } \left| -\frac{1}{2} \right\rangle, \quad (11)$$

in the upper left quadrant, i.e., when $h_L < 0$ and $h_R > 0$ and

$$\left| +\frac{1}{2} \right\rangle, \quad (12)$$

in the lower left quadrant when $h_L < 0$ and $h_R < 0$.

B. Ground state for the even number of sites

In this case, the spins of the ground states are always integers. As shown in Fig. 1 in the upper right quadrant, i.e., when both $h_{L(R)} > 0$, the ground state is doubly degenerated [43] and have total spins $S^z = 0, -1$ represented by

$$|0\rangle \text{ and } |-1\rangle. \quad (13)$$

The double degeneracy of the ground state is due to the presence of spin- $\pm 1/2$ spinons with infinite rapidity. These spinons have to be added *on top* of a background static spin configuration contributing to a total spin $-1/2$ in such a way that the total spins of the ground states are integers $S^z = 0, -1$. Using the isometry (2) we deduce immediately that in the lower left quadrant the ground states are given by

$$|0\rangle \text{ and } |+1\rangle \quad (14)$$

and also contain spin- $\pm 1/2$ spinons with infinite rapidity on top of a background spin- $1/2$ configuration. This is to be true independently of the magnitudes of the fields $|h_{L(R)}|$. When the boundary fields point towards opposite direction, like in the two upper left and lower right quadrants the ground state is unique with total spin $S^z = 0$,

$$|0\rangle \quad (15)$$

and do not contains spinons.

As we have seen the ground-state phase diagram exhibits four distinct phases depending solely on the orientations of the boundary fields. In each of the four quadrants defined by the sign of h_L and h_R , the ground-state degeneracy depends on the parity of N . It is twofold degenerate when $h_L h_R < 0$ for N odd and when $h_L h_R > 0$ for N even. In all other cases the ground state is nondegenerate contrary to what was found in [32]. Overall, our understanding of the spin quantum numbers in the different phases relies on a static background spin distribution on top of which spins $\pm 1/2$ spinons may or may not be added. Independently of the parity of the number of sites N , the background spin distribution contributes to a total spin $S_B^z = -\text{sgn}(h_L) 1/2$ when $h_L h_R > 0$, whereas $S_B^z = 0$ in the opposite case when $h_L h_R < 0$. Such a background spin structure is due to the presence of the boundary fields h_L and h_R , which are expected to induce a spin accumulation close to the edges. We shall return to this point in Sec. IV when we shall study the ground-state properties in more detail. For the time being, we shall argue that the phase structure induced by the presence of the boundary fields is much richer than the one we have just presented. When considering the whole structure of the Hilbert space, which calls for a detailed description of the excited states, we shall show that each of the four quadrants, ($h_L \geq 0, h_R \geq 0$), splits into four distinct subphases where the excited states organizes into different towers. This is the consequence of the well-known fact that the edge fields, when large enough, induce boundary bound states that are exponentially localized close to the edges.

III. EXCITED STATES

Before going into the description of the full solution of (5), let us review quickly how, in the case of a periodic chain without fields, the structure of the excitation spectrum depends on the parity of the number of sites N . When N is *even* the ground state is a singlet and the excitations are obtained by adding an *even* number of propagating holes or spinons. The spinons carry spins $\pm 1/2$ and have energy (8). Since physical excitations correspond to flipping a certain number of spins in the chain they carry integer spins $S^z \in \mathbb{Z}$ and therefore the spinons always come in pairs in an even chain. For the spin chain with an *odd* number of sites, the ground state is twofold degenerate with total spins $S^z = \pm 1/2$. Each of the ground states contains a spinon, with zero energy in the thermodynamical limit, and rapidity $\theta \rightarrow \infty$. In contrast with the even chain case, single spinon excitations with a finite rapidity, i.e., $\theta \neq \infty$, and energy (8) are allowed when N is odd. All other excitations are then obtained by adding an even number of spinons to the above states. Hence the total number of spinons in the odd spin chain is always an odd integer.

This scheme is to be modified in an open chain with boundary fields for which the ground state and, more importantly, the very structure of the Hilbert space of excitations strongly depend on the boundary fields $h_{L/R}$. As we shall see, when the boundary fields are strong enough (i.e., when $|h_{L/R}| \geq 2$), their main effect is to stabilize bound states which are *localized* at either the left or the right edge. These bound states have a finite, i.e., nonzero, energy above the ground state,

$$m_{L,R} = \frac{2\pi}{\sin\left(\frac{\pi}{h_{L,R}}\right)}, \quad (16)$$

and carry a spin-1/2 which points *towards* the direction of the boundary field at each edge. In the one particle (spin flip) sector, the bound state wave function can be found exactly [30,31]. We find that the bound states at the left and the right edges are exponentially localized as $\sim e^{-\kappa_L x}$ and $\sim e^{-\kappa_R(N-x)}$ respectively (see Appendix B), where

$$\kappa_j = \ln(h_j + 1), \quad j = L, R. \quad (17)$$

When the bound states exist, they generate independent towers of excited states on top of the ground-state one. All these towers of states eventually span the whole Hilbert space.

We distinguish between three regions, or subphases, *A*, *B*, and *C* depending on the number of localized bound states in the spectrum. In the region *A*, both boundary field strengths exceed a critical value $|h_{L/R}| \geq 2$ and there exist two boundary bound states localized at both ends of the chain. Depending on the relative orientations of the fields $h_{L/R}$ with respect to the z axis we further distinguish between four subphases $A_{j=(1,2,3,4)}$. In the region *B*, only one boundary field strength exceeds the critical value and there exists a single boundstate, which is localized at either the left or the right edge. Taking into account the orientations of the fields we end up with eight subphases B_j $j = (1, \dots, 8)$. Finally in region *C*, both $|h_{L/R}| < 2$ and there are no localized bound states; the four subphases $C_{j=(1,2,3,4)}$ account for all possible boundary fields orientations. The phase diagram is depicted in Fig. 2.

In the following, we shall present our results for the ground states as well as the Hilbert space structures in each phase.

Since, as with the PBC case discussed above, the spectral properties are very sensitive to the evenness of the number of sites N , we shall discuss separately both even and odd chains.

A. A subphases

We start with the *A* subphases where two boundary bound states are stabilized. The four $A_{j=(1,2,3,4)}$ subphases correspond to the domains of boundary fields $(h_L \geq 2, h_R \geq 2)$, $(h_L \leq -2, h_R \geq 2)$, $(h_L \leq -2, h_R \leq -2)$, and $(h_L \geq 2, h_R \leq -2)$, respectively. In the following we shall distinguish between odd end even chains and discuss separately the subphases $A_{j=(1,3)}$ and $A_{j=(2,4)}$.

1. Odd number of sites

The A_1 and A_3 subphases. In these cases, both boundary magnetic fields point towards the same direction: along the positive z axis for the A_1 subphase and negative z axis for the A_3 subphase. Both cases are related by the isometry (2). Qualitatively speaking, in the subphases $A_{1,3}$ and for N odd, the boundary magnetic fields are not frustrating in the sense that in the Ising limit of (1) the ground state would exhibit perfect antiferromagnetic order.

In the A_1 subphase, we find that the ground state is unique and has a total spin $S^z = -1/2$. We accordingly label the ground state in this phase by

$$\left| -\frac{1}{2} \right\rangle \quad (18)$$

and denote by E_0 its energy. The expression of E_0 as a function of $h_{L,R}$ is given in the Appendix [see Eq. (A7)]. We notice that due to the presence of the boundary fields the spin $-1/2$ of the ground state is not carried by a spinon in contrast with the periodic chain with N odd. It is rather the consequence of a static spin density distribution. We shall discuss this topic in more detail in the next section. Similarly to the case of periodic boundary conditions, one can build up excitations in the bulk on top of this ground state by adding an arbitrary *even* number of spinons, bulk strings and quartets [44,45]. These bulk excitations built on top of the state $\left| -\frac{1}{2} \right\rangle$ form a tower of excited states that we shall denote the ground-state tower.

As said above in the *A* subphases, there exists two boundary bound-state solutions exponentially localized at either the left or the right edge. In the language of the Bethe ansatz, they correspond to purely imaginary solutions of (5) (see Appendix A). These bound states carry a spin-1/2, whose spin orientation is along the boundary fields at each edge, and have an energy (4) Since the bound states carry a spin half, in order to add a bound state to the ground-state one also needs to add a spinon. This spinon may have spin $+1/2$ or $-1/2$ and an arbitrary rapidity θ . The energy cost in the process is

$$E_0 + m_{L,R} + E_\theta \quad (19)$$

and is minimal when $\theta \rightarrow \infty$. The corresponding states

$$\left| \pm \frac{1}{2} \right\rangle_L \text{ and } \left| \pm \frac{1}{2} \right\rangle_R, \quad (20)$$

have total spins $S^z = \pm 1/2$ and energies $E_0 + m_L$ and $E_0 + m_R$. The lowest excited states above (20) consist of spinon branches with energies given by (19) and $\theta \neq \infty$. On top of these, the states (20) generate, each, a tower of excited states obtained by adding an arbitrary *even* number of spinons, bulk

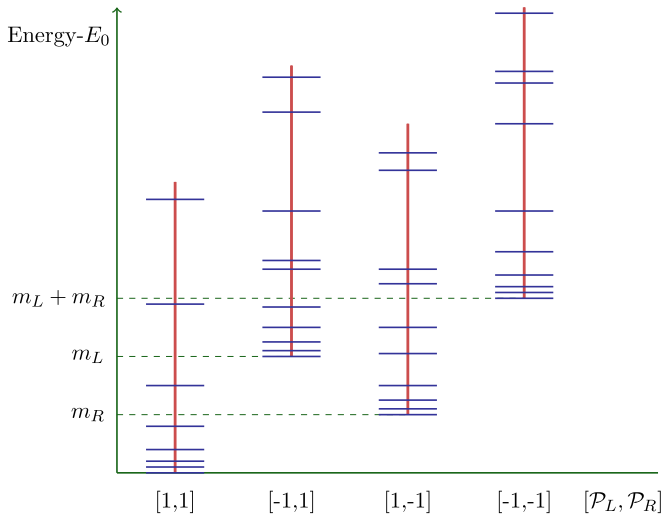


FIG. 4. Structure of the Hilbert space in the A subphases. In each A_j ($j = 1, 2, 3, 4$) subphase, there exist four towers of excited states, each labeled by the bound state parities $[\mathcal{P}_L, \mathcal{P}_R]$. The lowest energy states in each tower have energies close to the dashed lines corresponding to the energies E_0 , $E_0 + m_L$, $E_0 + m_R$, and $E_0 + m_L + m_R$.

strings, and quartets [45]. In both the left and right towers, built upon (20), a localized bound state at the left and the right edges is present and the number of spinon excitations is always odd.

On top of the above three towers there exists a fourth one which correspond to states which host two bound states. The state with the lowest energy in this tower is obtained by adding a localized bound state at the left and the right edges to the ground state (18). Since in the process the total spin of the state is shifted by 1, no spinon is required. The resulting state

$$|\pm \frac{1}{2}\rangle_{LR}, \quad (21)$$

which has a total spin $S^z = 1/2$ and an energy $E_0 + m_L + m_R$, generates a tower of excited states that comprises an arbitrary even number of spinons, bulk strings and quartets [45]. The number of spinon states in the whole tower is always even. We thus see that, in the A_1 subphase, the whole Hilbert space can be split into four towers generated by the states (18), (20), and (21) as illustrated in Fig. 4. On top of the ground-state tower which governs the low-energy physics, the remaining three towers contain at least one bound state at the edges and are high-energy states. In particular, we notice that in the A_1 subphase there exists excitations which contain a single spinon, and although the system is massless, their minimum energy is greater than the boundary gap m_L or m_R . These four towers can be labeled by the bound state parities

$$\mathcal{P}_{L,R} = (-1)^{\mathcal{N}_{L,R}}, \quad (22)$$

where $\mathcal{N}_{L,R}$ correspond to number of bound states at the left and right edges, respectively.

The situation in the A_3 subphase can be described in the very same way as above. Using the isometry (2), we can obtain all the states in the subphase A_3 starting from the states in the subphase A_1 by reversing the sign of the total spin S^z of the states. Hence, we obtain four towers of states in the subphase

A_3 generated by the states $|\pm \frac{1}{2}\rangle$, $|\pm \frac{1}{2}\rangle_{L,R}$ and $|\pm \frac{1}{2}\rangle_{LR}$ at energies E_0 , $E_0 + m_{L,R}$ and $E_0 + m_L + m_R$.

The A_2 and A_4 subphases. In these cases the boundary fields are frustrating for N odd in the sense discussed above. As we shall see in these subphases the Hilbert space is also split into four towers of states corresponding to the presence of boundary bound states. However, since the boundary magnetic fields at the two edges point toward opposite directions, the nature of these towers differ from the ones described above. Consider for instance the A_2 subphase in which the left boundary field points towards the negative z axis while the one at the right boundary points in the opposite direction. In this case we find that the ground state is twofold degenerated, each one containing a spinon (but no bound state) with spin $\pm 1/2$ and rapidity $\theta \rightarrow \infty$. These two states, i.e.,

$$|\pm \frac{1}{2}\rangle, \quad (23)$$

have total spin $S^z = \pm 1/2$ corresponding to the spin of the spinon, and generate a tower of excited state. It is obtained by adding an arbitrary even number of spinons, bulk strings, and quartets [45] on top of the two spin $\pm 1/2$ massless spinons branches with spectrum (8) and rapidity $\theta \neq \infty$. In contrast with the $A_{1,3}$ subphases, the ground-state tower contains an odd number of spinons.

Just as in the subphase A_1 , there exists two boundary bound-state solutions one at each edge. The bound state's spin is always oriented along the boundary magnetic field. Hence, in the subphase A_2 the bound state localized at the left edge has spin $-1/2$ whereas the bound state localized at the right edge has spin $+1/2$. We find that in order to add the bound state at the left edge with spin $-1/2$ one has to remove the $-1/2$ spinon at $\theta = \infty$ in the $|\pm \frac{1}{2}\rangle$ ground state (23). The resulting state has total spin $S^z = -1/2$ and energy $E_0 + m_L$. Similarly adding a spin $+1/2$ bound state at the right edge requires to remove the spin- $1/2$ spinon from the ground state $|\pm \frac{1}{2}\rangle$ (23). The resulting state has total spin $S^z = +1/2$ and energy $E_0 + m_R$. The two states with a bound state at either the left or right edge

$$|\pm \frac{1}{2}\rangle_L \text{ and } |\pm \frac{1}{2}\rangle_R, \quad (24)$$

generate, each, a tower of excited states upon adding an arbitrary even number of spinons, bulk strings and quartets [45]. In these two towers, the number of spinons in every state is always even.

Finally, the fourth tower is obtained by adding a bound state at each edge to the two ground states (23). The total spin of the resulting state does not change since the two, left and right, bound states have opposite spins. We obtain the states

$$|\pm \frac{1}{2}\rangle_{LR}, \quad (25)$$

which have an energy $E_0 + m_L + m_R$ and generate a tower of excited states. It is obtained by adding even number of spinons, bulk strings and quartets [45]. In this tower, the number of spinons is always odd.

Using symmetry (2), we can obtain all the states in the subphase A_4 from the states in the subphase A_2 by reversing their spins. The Hilbert space in the subphase A_4 can be similarly sorted out in terms of four towers of states built upon the states

$|\pm\frac{1}{2}\rangle, |+\frac{1}{2}\rangle_L, |-\frac{1}{2}\rangle_R$, and $|\pm\frac{1}{2}\rangle_{LR}$ with energies $E_0, E_0 + m_{L,R}$, and $E_0 + m_L + m_R$.

2. Even number of sites

When the number of sites is even the frustrating effect of the magnetic fields is reversed as compared to the N odd case. The boundary fields are frustrating in subphases $A_{1,3}$ while nonfrustrating in the subphases $A_{2,4}$.

The A_1 and A_3 subphases. In the subphase A_1 , we find that the ground state is twofold degenerated. It does not contain bound states but does contain a spinon with rapidity $\theta \rightarrow \infty$ and spins $\pm 1/2$. Despite this, since N is even, the total spins of the two degenerate ground states have to be integers. Indeed, as it comes out from our exact solution the two ground states have total spins $S^z = 0$ and $S^z = -1$. Our interpretation of this fact is that the two ground states with spin $S^z = 0$ and $S^z = -1$ contain a spin $+1/2$ and a spin $-1/2$ spinon respectively on top of a static background spin $-1/2$ distribution corresponding to the ground state in A_1 subphase when N is odd. In the following, we denote these two ground states by

$$|0\rangle \text{ and } |-1\rangle. \quad (26)$$

The ground-state tower of excited states comprises spin $\pm 1/2$ massless spinon states with energy $E_0 + m_R + E_\theta$ and finite rapidity $\theta \neq \infty$. The rest of the tower is then obtained by adding an arbitrary even number of spinons, bulk strings, and quartets [45]. In this tower, the number of spinon states is always odd.

Starting from one of the two ground states (26), one may add a bound state at either the left or the right edge. To this end, one needs to remove the spin $\pm 1/2$ spinon. The resulting total spin is then the sum of the bound-state spin $+1/2$ with that of the static background spin $-1/2$ distribution mentioned above. As a result, we end up with two states of total spin $S^z = 0$. The corresponding states with the bound state at the left or the right edge are denoted

$$|0\rangle_L \text{ and } |0\rangle_R \quad (27)$$

and have energies $E_0 + m_L$ and $E_0 + m_R$. Each of these two states generates a tower of excited states. In these towers the number of spinon states is always even.

The fourth tower is obtained from the ground states (26) by adding a bound state at each edge. Since the change of total spin is 1 there is no need to add or remove a spinon. In the process, we obtain two degenerate states, with total spins $S^z = 1$ and 0 and energy $E_0 + m_L + m_R$,

$$|1\rangle_{LR} \text{ and } |0\rangle_{LR}, \quad (28)$$

that host spin $\pm 1/2$ spinons with infinite rapidity as in the ground states. The fourth tower of excited states comprises, as in the ground-state tower, spin $\pm 1/2$ spinon states. These states have energy $E_0 + m_L + m_R + E_\theta$ and are gapped high-energy states. The remaining states of this towers are then built up by adding an even number of spinons, bulk strings, and quartets [45]. The number of spinon states is always odd.

Similar to the odd number of sites case, using symmetry (2), we can obtain all the states in the phase A_3 starting from the states in the phase A_1 described above.

The A_2 and A_4 subphases. In the subphase A_2 , we find that the ground state is nondegenerated

$$|0\rangle \quad (29)$$

and has total spin $S^z = 0$ with energy E_0 . Starting from this ground state, we can add a bound state at the left edge with spin $-1/2$. As already emphasized one also needs to add a spinon, with infinite rapidity and zero energy, for the total spin shift to be an integer. Depending on the spinon spin, which can be either $\pm 1/2$, one ends up with two states

$$|-1\rangle_L, |0\rangle_L, \quad (30)$$

which have total spins $S^z = -1$ and 0 and energy $E_0 + m_L$. One may repeat the same line of arguments with the right edge paying attention that the bound-state spin in this case is $+1/2$. The resulting two states

$$|+1\rangle_R, |0\rangle_R, \quad (31)$$

hosting a bound state at the right edge have total spins $S^z = 1$ and $S^z = 0$ and energy $E_0 + m_R$. Each left and right states (30) and (31) generate two towers of excited states that comprise spin $\pm 1/2$ spinons with energies $E_0 + m_{L,R} + E(\theta)$. The rest of the towers are obtained by adding even number of spinons, bulk strings, and quartets [45].

The fourth tower is obtained from the ground state (29) by adding a bound state with spin $-1/2$ at the left edge and spin $+1/2$ at the right edge. No spinons are needed in the process and one ends up with a single state

$$|0\rangle_{LR}, \quad (32)$$

with total spin $S^z = 0$ and energy $E_0 + m_R + m_L$. The latter state generates also a tower of states with even number of spinons, bulk strings, and quartets [45].

Using the symmetry (2), similar to the odd number of sites case, we can obtain all the states in the subphase A_4 starting from the states in the subphase A_2 described above. The ground state and the lowest energy state corresponding to each tower in all the A subphases for odd and even number of sites chain are summarized in Tables I and II, respectively.

B. B phases

1. Odd number of sites

In the B_1 subphase, the ground state has total spin $S^z = -1/2$ which corresponds to a static spin distribution and is represented by

$$\left|-\frac{1}{2}\right\rangle. \quad (33)$$

Unlike in the A phases, there exists only a single boundary bound-state solution corresponding to the bound state at the left edge. Starting from the ground state, this bound state can be added (which has spin $S^z = 1/2$) by adding a spinon whose spin orientation can be either in the positive or negative z direction resulting in the state with total spin $S^z = \pm 1/2$, respectively. This state has energy $E_0 + m_L + E_\theta$ and hence has the lowest energy in the limit $\theta \rightarrow \infty$. It is represented by

$$\left|\pm\frac{1}{2}\right\rangle_L. \quad (34)$$

TABLE I. Energies and bound state parities of the ground state and the lowest energy states corresponding to each tower in all the A subphases for odd number of sites is shown below. The subscripts L, R denote the location of the bound states at the left or the right boundary.

Phase	State	Energy- E_0	\mathcal{P}_L	\mathcal{P}_R
A_1	$ \frac{1}{2}\rangle$	0 (g.s)	1	1
	$ \pm\frac{1}{2}\rangle_R$	m_R	1	-1
	$ \pm\frac{1}{2}\rangle_L$	m_L	-1	1
	$ \frac{1}{2}\rangle_{L,R}$	$m_L + m_R$	1	1
A_3	$ \frac{1}{2}\rangle$	0 (g.s)	1	1
	$ \pm\frac{1}{2}\rangle_R$	m_R	1	-1
	$ \pm\frac{1}{2}\rangle_L$	m_L	-1	1
	$ \frac{1}{2}\rangle_{L,R}$	$m_L + m_R$	1	1
A_2	$ \frac{1}{2}\rangle$	0 (g.s)	1	1
	$ \pm\frac{1}{2}\rangle$	0 (g.s)	1	1
	$ \pm\frac{1}{2}\rangle_{L,R}$	$m_L + m_R$	-1	-1
	$ \frac{1}{2}\rangle_R$	m_R	1	-1
A_4	$ \frac{1}{2}\rangle$	0 (g.s)	1	1
	$ \pm\frac{1}{2}\rangle_R$	m_R	1	-1
	$ \pm\frac{1}{2}\rangle$	0 (g.s)	1	1
	$ \pm\frac{1}{2}\rangle_{L,R}$	$m_L + m_R$	-1	-1
	$ \frac{1}{2}\rangle_L$	m_L	-1	1

In the subphase B_2 , the state which does not contain a bound state at either edge contains a spinon whose spin orientation is either in the positive or negative z direction. The energy of this state is $E_0 + E_\theta$ and thus forms a continuous branch parameterized by θ . The ground state is obtained in

TABLE II. Energies and bound state parities of the ground state and the lowest energy states corresponding to each tower in all the A subphases for even number of sites is shown below.

Phase	State	Energy- E_0	\mathcal{P}_L	\mathcal{P}_R
A_1	$ -1\rangle, 0\rangle$	0 (g.s)	1	1
	$ 0\rangle_R$	m_R	1	-1
	$ 0\rangle_L$	m_L	-1	1
	$ 1\rangle_{L,R}, 0\rangle_{L,R}$	$m_L + m_R$	1	1
A_3	$ 1\rangle, 0\rangle$	0 (g.s)	1	1
	$ 0\rangle_R$	m_R	1	-1
	$ 0\rangle_L$	m_L	-1	1
	$ -1\rangle_{L,R}, 0\rangle_{L,R}$	$m_L + m_R$	1	1
A_2	$ 0\rangle$	0 (g.s)	-1	-1
	$ -1\rangle_L, 0\rangle_L$	m_L	1	-1
	$ 1\rangle_R, 0\rangle_R$	m_R	-1	1
	$ 0\rangle_{L,R}$	$m_L + m_R$	1	1
A_4	$ 0\rangle$	0 (g.s)	-1	-1
	$ 1\rangle_L, 0\rangle_L$	m_L	1	-1
	$ -1\rangle_R, 0\rangle_R$	m_R	-1	1
	$ 0\rangle_{L,R}$	$m_L + m_R$	1	1

the limit $\theta \rightarrow \infty$ and is represented by

$$|\pm\frac{1}{2}\rangle \quad (35)$$

Starting from this ground state, one can add a bound state at the left edge (which has spin $S^z = -1/2$) by removing the existing spinon. The resulting state has energy $E_0 + m_L$ with total spin $S^z = -1/2$ and is represented by

$$|\frac{1}{2}\rangle_L. \quad (36)$$

By using the transformation $L \rightarrow R$, the states in the phases B_8 and B_7 can be obtained by starting with the states in the phases B_1 and B_2 , respectively. By using the transformation (2), the states in the phases B_5 , B_6 , B_3 , and B_4 can be obtained from the states in the phases B_1 , B_2 , B_7 , and B_8 , respectively.

2. Even number of sites

In the phase B_1 , the state with no bound states at both the edges is twofold degenerate. It contains a spinon on top of the static spin distribution of the ground state in the phase B_1 corresponding to odd number of sites case. The spin orientation of the spinon can be either in the positive or negative z direction which results in a doubly degenerate state with total spin $S^z = 0, -1$. This state has energy $E_0 + E_\theta$ and thus forms a continuous branch which is parameterized by θ . The ground state is obtained in the limit $\theta \rightarrow \infty$ and is represented by

$$|0\rangle, |-1\rangle. \quad (37)$$

We can add the bound state at the left edge (with spin $S^z = 1/2$) to the ground state by removing the existing spinon. This results in a state

$$|0\rangle_L \quad (38)$$

with total spin $S^z = 0$ with energy $E_0 + m_L$.

In the phase B_2 , the state which does not contain bound state at either edge has total spin $S^z = 0$ and has energy E_0 . It is represented by

$$|0\rangle. \quad (39)$$

We can add the bound state at the left edge (with spin $S^z = -1/2$) by adding a spinon with spin oriented either in the positive or negative z direction and hence resulting in a doubly degenerate state with total spin $S^z = -1, 0$. This state has energy $E_0 + E_\theta + m_L$, and hence the lowest energy of this state corresponds to the limit $\theta \rightarrow \infty$ and is represented by

$$|0\rangle_L, |-1\rangle_L. \quad (40)$$

Similar to the odd number of sites case, the states in the phases B_8 and B_7 can be obtained by starting with the states in B_1 and B_2 , respectively, by making the transformation $L \rightarrow R$. By using transformation (2), the states in the phases B_5 , B_6 , B_3 , and B_4 can be obtained from the states in the phases B_1 , B_2 , B_7 , and B_8 , respectively. Unlike in the A subphases where there exists bound states at both the edges, we have seen that in B subphases there exists only one bound state at either the left or the right edge. Similar to the A subphases, excitations can be built up starting from the ground state and from the state containing a bound state either at the left or the right edge by adding even number of spinons, strings and quartets [45]. This leads to the Hilbert space in each B

TABLE III. Energies and local bound state parities of the ground state and the lowest energy states corresponding to each tower in all the B phases for odd number of sites is shown below.

Phase	State	Energy- E_0	\mathcal{P}_L	\mathcal{P}_R
B_1	$ \frac{-1}{2}\rangle$	0 (g.s)	1	1
	$ \pm\frac{1}{2}\rangle_L$	m_L	-1	1
B_8	$ \frac{-1}{2}\rangle$	0 (g.s)	1	1
	$ \pm\frac{1}{2}\rangle_R$	m_R	1	-1
B_2	$ \frac{-1}{2}\rangle_L$	m_L	-1	1
	$ \pm\frac{1}{2}\rangle$	0 (g.s)	1	-1
B_7	$ \pm\frac{1}{2}\rangle$	0 (g.s)	1	1
	$ \frac{-1}{2}\rangle_R$	m_R	1	-1
B_4	$ \frac{1}{2}\rangle$	0 (g.s)	1	1
	$ \pm\frac{1}{2}\rangle_R$	m_R	1	-1
B_5	$ \frac{1}{2}\rangle_L$	0 (g.s)	1	1
	$ \pm\frac{1}{2}\rangle_L$	m_L	-1	1
B_3	$ \pm\frac{1}{2}\rangle$	0 (g.s)	1	1
	$ \frac{1}{2}\rangle_R$	m_R	1	-1
B_6	$ \pm\frac{1}{2}\rangle$	0 (g.s)	1	1
	$ \frac{1}{2}\rangle_L$	m_L	-1	1

subphase consisting of only two towers. For example, in the phase B_1 , the two towers have the bound state parities $\mathcal{P}_L = 1$, $\mathcal{P}_R = 1$ and $\mathcal{P}_L = -1$, $\mathcal{P}_R = 1$, whereas in the B_8 phase they correspond to $\mathcal{P}_L = 1$, $\mathcal{P}_R = 1$ and $\mathcal{P}_L = 1$, $\mathcal{P}_R = -1$. The ground states and the lowest energy states corresponding to the two towers in all the B subphases are summarized in Tables III and IV.

C. C subphases

Odd number of sites. In the subphases C_1 and C_3 , the ground state is represented by

$$|\mp\frac{1}{2}\rangle \quad (41)$$

and have total spin $S^z = \mp 1/2$ respectively, which corresponds to a static spin distribution. In the subphases C_2 and C_4 the lowest energy state contains a spinon with spin pointing either in the positive or negative z direction resulting in a twofold degenerate state parameterized by rapidity θ . The ground state is obtained in the limit $\theta \rightarrow \infty$. The spin orientation of the spinon dictates the total spin $S^z = \pm 1/2$ of the state. They are represented by

$$|\pm\frac{1}{2}\rangle. \quad (42)$$

Even number of sites. In the subphase C_1 , the lowest energy state contains a spinon with rapidity θ with spin oriented either in the positive or negative z direction on top of the static spin distribution of the ground state in the subphase C_1 corresponding to odd number of sites case. This state is twofold degenerate and is parameterized by rapidity θ . The ground state is obtained in the limit $\theta \rightarrow \infty$ and is

TABLE IV. Energies and local bound state parities of the ground state and the lowest energy states corresponding to each tower in all the B phases for even number of sites is shown below.

Phase	State	Energy- E_0	\mathcal{P}_L	\mathcal{P}_R
B_1	$ -1\rangle, 0\rangle$	0 (g.s)	1	1
	$ 0\rangle_L$	m_L	-1	1
B_8	$ -1\rangle, 0\rangle$	0 (g.s)	1	1
	$ 0\rangle_R$	m_R	1	-1
B_2	$ -1\rangle_L, 0\rangle_L$	m_L	-1	1
	$ 0\rangle$	0 (g.s)	1	1
B_7	$ -1\rangle_R, 0\rangle_R$	m_R	1	-1
	$ 0\rangle$	0 (g.s)	1	1
B_4	$ 1\rangle, 0\rangle$	0 (g.s)	1	1
	$ 0\rangle_R$	m_R	1	-1
B_5	$ 1\rangle, 0\rangle$	0 (g.s)	1	1
	$ 0\rangle_L$	m_L	-1	1
B_3	$ 1\rangle_R, 0\rangle_R$	m_R	1	-1
	$ 0\rangle$	0 (g.s)	1	1
B_6	$ 1\rangle_L, 0\rangle_L$	m_L	-1	1
	$ 0\rangle$	0 (g.s)	1	1

represented by

$$|0\rangle, |-1\rangle \quad (43)$$

with total spin $S^z = 0$ and -1 corresponding to the spin orientation of the spinon which is along the positive and negative z directions, respectively. Similarly, in the subphase C_3 , the lowest energy state contains a spinon with spin pointed either in the positive or negative z direction with rapidity θ on top of the static spin distribution of the ground state in the phase C_3 corresponding to odd number of sites case. It is twofold degenerate and is parameterized by rapidity θ . The ground state is obtained in the limit $\theta \rightarrow \infty$ and is represented by

$$|0\rangle, |1\rangle \quad (44)$$

with total spin $S^z = 0$ and 1 corresponding to the spin orientation of the spinon which is along the negative and positive z directions, respectively. In the subphases C_2 and C_4 , the ground state has total spin $S^z = 0$ and is represented by

$$|0\rangle. \quad (45)$$

Similar to the A and B subphases, in each C subphase, excitations can be built on top of the ground state by adding even number of spinons, strings, and quartets [45] generating a single tower of excited states which can be labeled by $\mathcal{P}_L = 1, \mathcal{P}_R = 1$.

D. Boundary eigenstate phase transition

After this rather lengthy, but complete, description of the excited states let us now summarize our results. As we saw there exists a critical value of the edge fields h_c , $|h_c| = 2$, at each edge associated with the existence of an edge bound state. When $|h_{i=(L,R)}| > 2$ a localized bound state is stabilized

close to the corresponding edge $i = (L, R)$. The three types of phases A_j , B_j , and C_j distinguish themselves by the number of bound states they support, i.e., two, one, and zero. Independently of the parity of N , we showed that in the A -type phases the Hilbert space splits into four towers of excited states while there exists two towers in the B -type phases and only one tower in the C -type phases. When compared to the ground-state phase diagrams [see Figs. 1 and 3] each quadrant splits into one C_j subphase, two B_j subphases and one A_j subphase as displayed in the Fig. 2. At this point a natural question arises: what is the nature of the transition that occurs as one moves from an A_j subphase to a B_j subphase or from a B_j subphase to a C_j subphase by varying the edge fields.

Without loss of generality let us fix on quadrant with $h_L > 0$ and $h_R > 0$. Consider first the situation where both $h_{L(R)} > 2$, that is one sits in the A_1 subphase. Then let the left boundary magnetic field h_L be fixed while the right boundary fields h_R is decreased. As h_R is decreased below the critical value $h_c = 2$, we move into the subphase B_1 . The two states which contain the bound state at the right edge no longer exist. On the boundary between the A_1 and B_1 subphases, the energy of the bound state and energy of the spinon with zero rapidity coincide $m_R \sim 2\pi = E_{\theta \rightarrow 0}$. Hence it is natural to interpret that the bound state at the right edge leaks into the bulk by taking the form of a spinon with rapidity $\theta \sim 0$. Similarly, moving from A_1 to B_8 (see Fig. 2), the bound state corresponding to left boundary leaks into the bulk. Similarly, moving from B_1 to C_1 , the value of the left boundary field takes values lesser than critical value, and hence the bound state present at the left edge leaks into the bulk in a similar way, resulting in C_1 having no bound states at either edge. The same phenomena of bound states leaking into the bulk occurs as one moves from any A subphase into the respective B and C subphases.

More importantly, associated with the appearance or disappearance of localized bound states is the fact that when one goes from any subphase to another, the whole structure of the Hilbert space changes. The excited states organize themselves into towers whose number is different in the A , B , or C type phases. We saw that the towers are labeled by additional quantum numbers which are the bound state parities $\mathcal{P}_{L,R}$ [see Eq. (22)]. The four towers in A -type phases are labeled by $(\mathcal{P}_L, \mathcal{P}_R) = (\pm 1, \pm 1)$, the two towers in the B -type phases by $(\mathcal{P}_L, \mathcal{P}_R) = (\pm 1, +1)$ and $(\mathcal{P}_L, \mathcal{P}_R) = (+1, \pm 1)$ and the unique tower of the C -type phases by $(\mathcal{P}_L, \mathcal{P}_R) = (+1, +1)$. It is interesting to notice that one may have also labeled these towers in the A -type phases by the spinon parity $\mathcal{P}_s = (-1)^n$, where n denotes the number of spinons in a given eigenstate of the Hamiltonian. The relation between \mathcal{P}_L , \mathcal{P}_R and \mathcal{P}_s depends on the phase and the parity of the number of sites N as follows:

$$\mathcal{P}_L \mathcal{P}_R (-1)^n (-1)^N = (-1)^k, \quad (46)$$

where k labels the different subphases A_k as given in Fig. 2. As when crossing from an A_j subphase to either a B_j or C_j subphase the structure of the Hilbert space changes, as illustrated in Fig. 5, and we coin the corresponding phase transition a boundary eigenstate phase transition. Such transitions might be probed through dynamical properties at infinite temperatures that involve operators localized close enough to the boundaries. We shall elaborate on this topic in a forthcoming

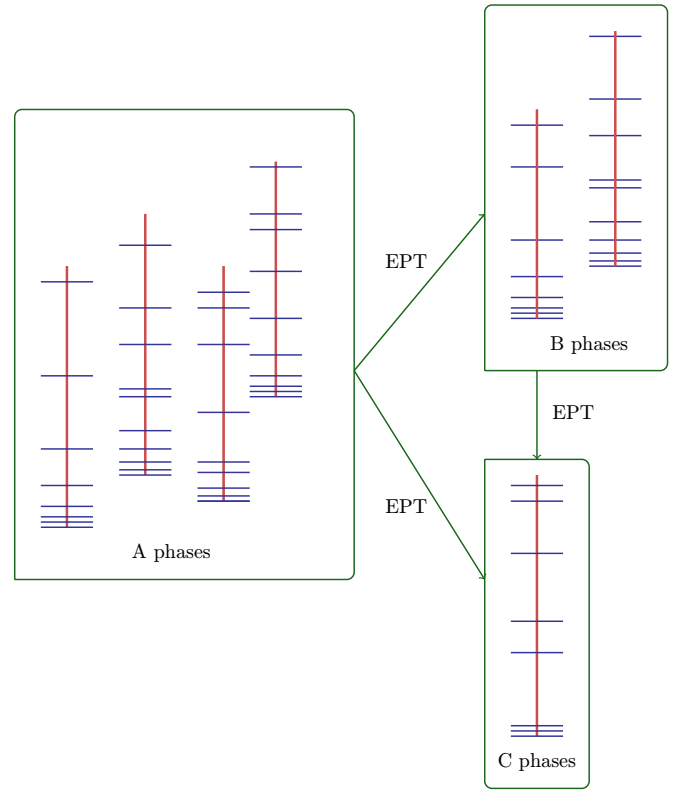


FIG. 5. Hilbert space in the A phases is comprised of four towers whereas it is comprised of two towers in the B phases and a single tower in the C phases. Figure illustrates the boundary eigenstate phase transitions (BEPT) that occur between A , B , and C type phases, where the number of towers of the Hilbert space changes.

work. At present, we shall content ourselves, in the next section, with the simpler question of how this transition reflects itself in the ground-state properties of local observables.

IV. GROUND-STATE MAGNETIZATION PROFILE AND SPIN ACCUMULATION

To this end, we shall be interested in the behavior of the *local* magnetization profile induced by the edge magnetic fields in the different subphases. We shall use the DMRG method, which is ideal for one-dimensional systems, to calculate the ground state of Eq. (1) on finite size systems. In particular, we considered system sizes up to $N = 1600$ sites, where a maximum of 1000 states are kept to keep the truncation error below 10^{-12} . The DMRG calculations in this paper are performed using the ITENSOR library [46]. Once the ground state is obtained we compute the spin expectation value $S^z(x_i) \equiv \langle \sigma_i^z / 2 \rangle$ as a function of position x_i for various edge magnetic fields h_L, h_R in the different phases of the problem.

A. Magnetization profile

From the magnetization obtained from the DMRG calculations, we use the following ansatz for the magnetization near the boundary:

$$S^z(x_i) = (-1)^i \left(A + \frac{B}{\sqrt{x_i}} + C e^{-x_i/\xi} \right) + \frac{D}{x_i}. \quad (47)$$

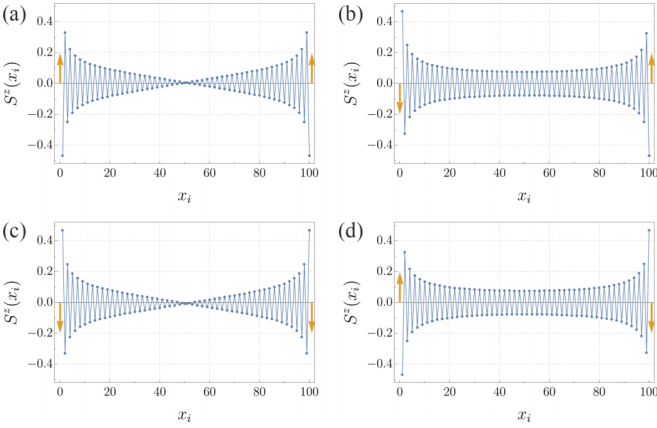


FIG. 6. Magnetization profile of the ground state in (a) A_1 , (b) A_2 , (c) A_3 , and (d) A_4 phases, respectively. The boundary fields are $h_L = \pm 4$, $h_R = \pm 4$ on a chain of length $N = 100$, and the arrow indicates the direction of the boundary fields.

We have introduced a constant staggered magnetization (A) that vanishes in the thermodynamic limit as well as the alternating $1/\sqrt{x}$ and uniform $1/x$ terms which account, to leading order, for the gapless bulk. In the bosonization language, they correspond to the staggered and uniform component of the magnetization in the long-distance limit. In addition to the above terms, we have also included a term which goes like $\sim e^{-x_i/\xi}$ to account for any exponentially localized spin accumulation.

Overall we find excellent agreement between our DMRG results and its fit (47) for several values of h_L and h_R . We show in Fig. 6, as an example, the magnetization profile $S^z(x_i)$ deep in four A phases for the boundary fields $|h_L| = |h_R| = 4$ and system size $N = 100$. As expected, the magnetizations at the boundaries are all opposite to the boundary field directions and one clearly observes a spin accumulation close to the edges. We notice though that since the bulk is gapless, the spin accumulation is not expected to be sharply localized at the edge. This can be seen in the magnetization profile which exhibit asymptotic power-law antiferromagnetic decay sufficiently far away from the edges. Notice that, since in the A_1 and A_3 phases, the ground state contains a spinon in the bulk for even chains, a node in the bulk antiferromagnetic

configuration [Figs. 6(a) and 6(c)] is clearly seen. Alternatively, for odd chain lengths the A_1 and A_3 phases have no spinons whereas the A_2 and A_4 phases do. We now discuss in more detail about our results for the fit in the particular case $h_L = h_R = h$, where the system exhibits a \mathbb{Z}_2 space parity symmetry. As one varies h , this allows us to study the spin magnetization profile when going from the C_1 phase to the A_1 phase (see Fig. 2). We show for example in Fig. 7(a) the magnetization profile for different values of h in the A_1 phase and the critical point. Fitting the DMRG data with the form (47), we can extract the parameters A , B , C , and D as well as the length scale ξ as a function of h . The coefficients C of the exponential term and D of the uniform component $1/x$ are shown in Fig. 7(b). The constant term A and the coefficient B of the staggered magnetization component $1/\sqrt{x}$ are shown in Fig. 8(b). Finally ξ is shown in Fig. 8(c).

From our data, we first observe that when $h = h_c = 2$ the magnetization profile takes a particular simple form in the thermodynamical limit

$$S^z(x_i) \simeq (-1)^i 0.413/\sqrt{x_i}, \quad (48)$$

as both C and D are zero (even at a finite size) and A goes to zero as $N \rightarrow \infty$. We display in Fig. 8(a) our best fit for the magnetization when $h = h_c = 2$ and $N = 1000$, which shows an almost perfect $\sim 1/\sqrt{x}$ behavior asymptotically. It is remarkable that for this value of the edge field the bulk uniform component $1/x$ disappears from the magnetization profile.

This case $h = h_c = 2$ seems to play a special role in the magnetization profile. Indeed we find that both the coefficient C and D change sign when going across the $h = h_c = 2$ point where they vanish. The change in the sign of C means that the exponential term enhances (diminishes) its contribution to $S^z(x_i)$ when $h > h_c$ ($h < h_c$). On the other hand the change of sign of D can be interpreted as a π phase shift of the uniform component term in Eq. (47). At the transition, both contributions vanish as we find $C, D = 0$. Another important feature is that coefficients A and B saturate as one increases h above $h_c = 2$ as seen in Fig. 8(b). This means that at magnetic fields h larger than $h_c = 2$ the constant contribution as well as the staggered component of the magnetization are insensitive to the edge magnetic field. As these are the dominant contributions for large x , this means that the magnetizations far from the edges are essentially insensitive to the edge fields when

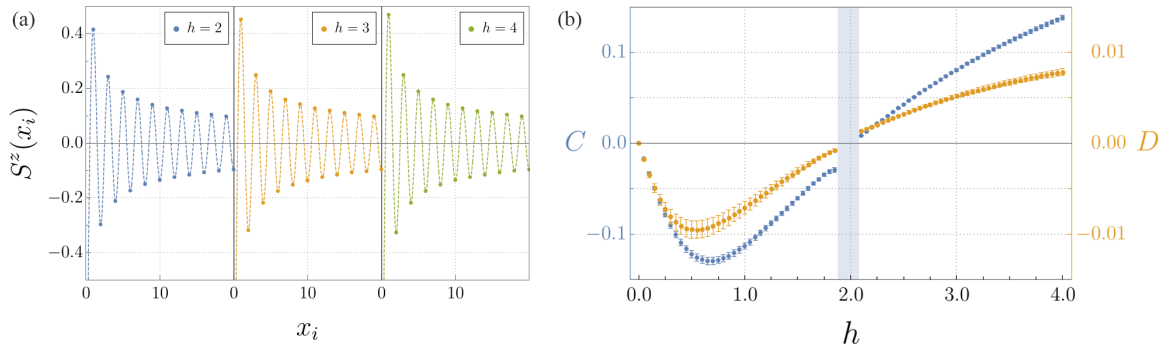


FIG. 7. (a) Magnetization (dots) and its fit to Eq. (47) (dashed lines) for the first 20 sites of $N = 1000$ chain. (b) The fit parameters C and D from Eq. (47), as a function of h . Both parameters vanishes at the critical $h_c = 2$. The shaded region is where the fitting to Eq. (47) numerically fails as it is close to $h_c = 2$. (See Appendix C for more details.)

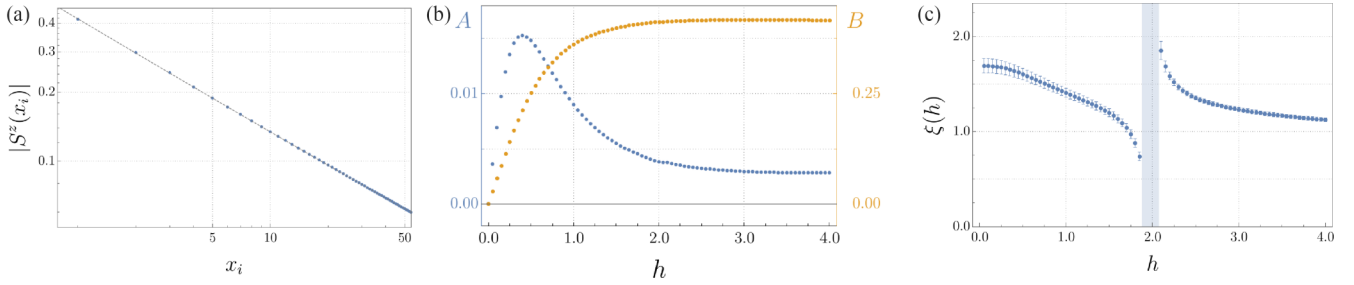


FIG. 8. (a) Magnetization for the $N = 1000$ chain with critical boundary fields ($h = h_c = 2$). The magnetization of a critical chain decays as $\sim 1/\sqrt{x_i}$ as can be seen from the good agreement with the $|S^z(x_i)| = 0.413/\sqrt{x_i} + 0.00385$ obtained from fitting the data. (b) The fit parameters A and B from Eq. (47), as a function of boundary field h . (c) The length scale ξ of the exponentially localized boundary spin, also from Eq. (47), as a function of h . The critical point is $h_c = 2$ where the length scale diverges.

$h > h_c$, in contrast to low fields $h < h_c$ where both A and B wildly varies.

In the light of the discussion given in the precedent section, it seems that at the critical point where the boundary eigenstate phase transition occurs (here between the A_1 and C_1 phases on the \mathbb{Z}_2 symmetric line $h_L = h_R$) a qualitative change also occurs in the magnetization profile in the ground state. Whether this change corresponds to a genuine critical point for the ground-state properties (reflecting itself into a singular behavior of the magnetization profile at h_c) is a nontrivial issue. Indeed, although we find that the length scale ξ diverges as h approaches h_c , at the same time $C, D \rightarrow 0$ and the numerical fitting overfits the data in the vicinity of the critical point ($h = h_c = 2$). We mark this region with a grey shade in Figs. 7(b) and 8(c) (for more detail see Appendix C). We therefore find it difficult to conclude that these coefficients, or length scale ξ , serve as order parameters for a genuine ground-state phase transition.

B. Boundary spin accumulation

Due to the edge magnetic fields we naturally expect that some amount of spin is getting accumulated close to the edges. To calculate the spin accumulation associated with the edges of the system, we use the following definition of the spin accumulation on the left boundary S_L^z as [47]

$$S_L^z = \lim_{\alpha \rightarrow 0} \lim_{N \rightarrow \infty} S_L^z(\alpha, N), \quad (49)$$

where

$$S_L^z(\alpha, N) = \sum_i e^{-x_i \alpha} S^z(x_i). \quad (50)$$

Note the order of the limit is relevant and it is important to take the thermodynamic limit first. Otherwise, the $\alpha \rightarrow 0$ limit removes the cutoff and the result becomes merely the total S^z of the system. Also, $\alpha \gg 1/L$ should be satisfied for the cutoff to be meaningful. In the following we shall compute S_L^z in both the C_2 and A_2 phases where $h_L = -h_R = -h$. The reason for this is to keep the odd parity of the system which simplifies the finite-size conjectures which will follow.

To obtain S_L^z systematically, we infer $\lim_{N \rightarrow \infty} S_L^z(\alpha, N) \equiv S_L^z(\alpha)$ from the finite size calculations. Figure 9(a) shows the $S_L^z(\alpha, N)$ as a function of α for different system sizes, when $h = 4$. One important observation is that, as the system size grows $S_L^z(\alpha, N)$ converges to the $S_L^z(\alpha)$ curve. Therefore, each

$S_L^z(\alpha, N)$ is converged to $S_L^z(\alpha)$ for α larger than a certain value of α_N , which $\lim_{N \rightarrow \infty} \alpha_N = 0$. We conjecture the leading difference of the finite $S_L^z(\alpha, N)$ and infinite $S_L^z(\alpha)$ as

$$S_L^z(\alpha) = S_L^z(\alpha, N) - \frac{1}{4} e^{-N\alpha} + \dots, \quad (51)$$

for $h \geq h_c$. This equation is suggestive that it consists of the proposed spin (1/4) and the only length scale (N) and directly implies the fractional 1/4 spin. Taking the $\alpha \rightarrow 0$ limit to Eq. (51), the first term vanishes because $S_L^z(0, N) = \sum_i S^z(x_i)$ for any finite N and the total S^z is zero for the even chain in A_2 phase. The remaining terms give the fractionalized $S_L^z = \pm 1/4$ per Eq. (49) where the sign depends on the direction of the boundary field.

To see how this work let us give an example of our finite size scaling procedure in the particular case $h = 4$. In Fig. 9(b), we plot $S_L^z(\alpha, 300) - S_L^z(\alpha, N)$ for various N for the same parameters in Fig. 9(a). As we expect from our conjecture [Eq. (51)], the difference converges to $\frac{1}{4} e^{-N\alpha}$ (dashed line) for large N . To quantify the numerical value of S_L^z , we find the best exponential fit to the plots similar to Fig. 9(b) for different h values, and obtain the spin accumulation $S_L^z(h)$ as the overall coefficient.

Our final result for the spin accumulation S_L^z as a function of h is shown in Fig. 9(c). Our results for S_L^z are consistent with $S_L^z = 1/4$ for $h \geq h_c = 2$ and decreases for smaller values of h . We thus find that at large fields $h \geq h_c = 2$ a fractional quarter spin is likely to be accumulated at the edge in the A_2 phase. The situation at hand is similar to what happens in topological one dimensional gapless Spin Triplet Superconductors (STS) where there also a fractional spin 1/4 is getting localized at the edge. However, in the present case, we do not expect S_L^z to be a sharp quantum observable in contrast with the STS case where eigenvalues of S_L^z label the different edge states of the system. The reason for this stems from the absence of a gap in the bulk of the Heisenberg chain in contrast with STS. The best way to check this is to compute the variance of the operator S_L^z [Eq. (49)]

$$\sigma_S^2 = \lim_{\alpha \rightarrow 0} \lim_{N \rightarrow \infty} \sigma_S^2(\alpha, N),$$

$$\sigma_S^2(\alpha, N) = \langle (S_L^z(\alpha, N))^2 \rangle - \langle S_L^z(\alpha, N) \rangle^2. \quad (52)$$

We show in Fig. 10(a) $\sigma_S^2(\alpha, N)$ for different system sizes and $h = 4$. We observe the $\sigma_S^2(\alpha, N)$ converges to $\sigma_S^2(\alpha)$ as

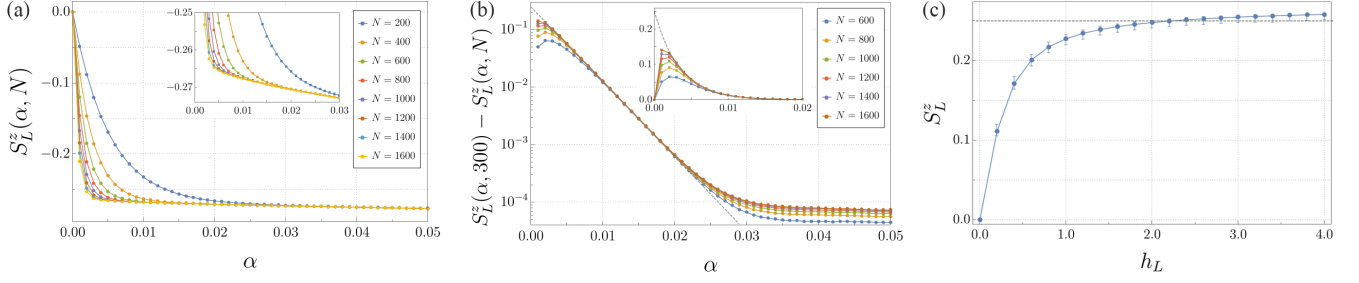


FIG. 9. (a) Spin accumulation $S_L^z(\alpha, N)$ for various system sizes when $h_L = -h_R = 4$. The inset is a blowup near $\alpha = 0$. (b) The difference between the spin accumulation for system size N and that of the system of $N = 300$. The inset is the same plot in linear scale, and the gray dashed lines are the conjectured $(1/4)e^{-300\alpha}$. (c) The boundary spin accumulation obtained from the linear fit of (b) to $Ae^{-300\alpha}$ as a function of boundary field h_L .

system size increases. We are thus led to conjecture the leading finite-size correction to the infinite N limit:

$$\sigma_S^2(\alpha) = \sigma_S^2(\alpha, N) + \frac{a}{(N\alpha)^2 + b} + \dots \quad (53)$$

This conjecture is based on the empirical observation that the difference of two curves in Fig. 10(a) follows $1/\alpha^2$ for large α and remains finite at $\alpha = 0$, which is qualitatively reminiscent of how the connected spin-spin correlation function (that the variance is related to) vanishes for large momentum (represented by α). Figure 10(b) shows $\Delta\sigma_S^2(\alpha, N) \equiv \sigma_S^2(\alpha, N) - \sigma_S^2(\alpha, 300)$, together with the fitted equations using Eq. (53). Importantly, we find that a and b are essentially independent of N (with discrepancies within 1.61%) demonstrating the quality of the conjectured functional form with only two fit parameters.

We again take the $\alpha \rightarrow 0$ limit of Eq. (53) and obtain σ_S^2 . Using the fitted parameters a and b from $\sigma_S^2(\alpha, 600) - \sigma_S^2(\alpha, 300)$, we get $\sigma_S^2 = \sigma_S^2(0, N) + a/b$. Since σ_S^2 and a/b does not depend on N , the remaining term $\sigma_S^2(0, N)$ should also be N independent. We indeed find that $\sigma_S^2(0, N)$ is nearly zero, and three orders of magnitude smaller than a/b . From this, we plot $\sigma_S^2(\approx a/b)$ as a function of h in Fig. 10(c). Although the variance decrease as h increase and crosses the phase transition, it remains nonzero. This means that S_L^z does not represent a sharp quantum observable, and as such, we cannot, in contrast with topological STS superconductor; label the states according to the value of the spin accumulations at the edges.

Overall we find that the ground-state properties, as probed by the magnetization profile, displays interesting and nontrivial behavior as a function of the edge fields h . In particular we observe that above the critical value $h > h_c = 2$ a fractional spin 1/4 is likely to be accumulated at the edge of the chain. However, in contrast with what happens in topological spin triplet superconductor, this fractional spin is not a sharp quantum observable and cannot be used as a genuine quantum number. The reason for this stems from the absence of a gap in the bulk. Nevertheless, the behavior of the spin accumulation as well as the change of the magnetization profile in the ground state might reflect, at least qualitatively, the boundary eigenstate phase transition between phases A and C discussed in the previous section.

V. DISCUSSION

We considered spin-1/2 Heisenberg chain with boundary magnetic fields and analyzed it analytically using Bethe ansatz and also numerically using DMRG. Although the Heisenberg chain has been immensely studied and is very well understood, the results that we have presented in this work have not been found before. We find that the system exhibits four different ground states for four different orientations of the boundary fields. The total spin S^z in each ground state may differ, which depends on the orientation of the boundary fields and also depends on the evenness or oddness of the number of sites of the chain. As the orientation of the magnetic fields is changed, the system undergoes a phase transition where the

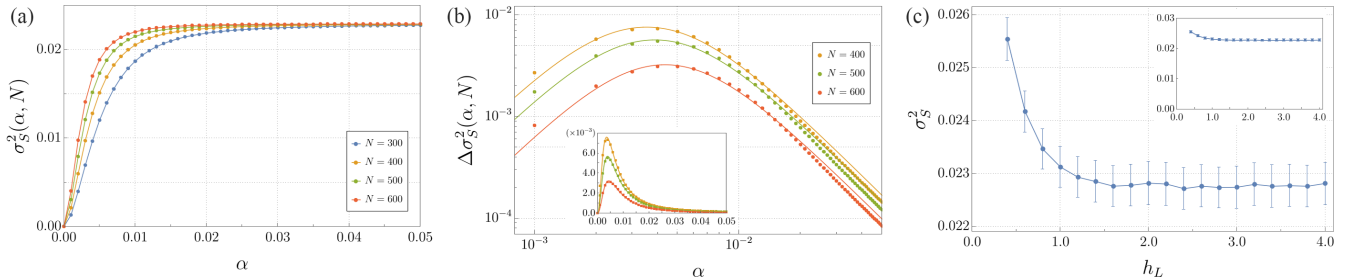


FIG. 10. (a) Variance of $S_L^z(\alpha, N)$ for various system sizes when $h_L = -h_R = 4$. (b) The difference between the variance for system size N and that of the system of $N = 300$. The linear behavior for large α in this log-log plot suggests the difference is asymptotically $\sim\alpha^{-2}$. The solid lines are the result of a fit based on Eq. (53). The discrepancies at large α are exaggerated due to the logarithmic scale. The inset is the same figure in linear scale which shows good agreement between data and fit. (c) The variance obtained by the fit parameters of (b). Variance remains nonzero beyond the phase transition. Inset is the same quantity plotted in a y-axis range down to zero.

ground state of the system changes. The nature of this phase transition is currently unknown to us and will be analyzed in the future work.

For a given orientation of the boundary fields, the system exhibits a high-energy bound state exponentially localized at an edge when the boundary magnetic field takes values greater than the critical field h_c . Every phase corresponding to a certain ground state can be further divided into four subphases. In one of the subphases, the system exhibits bound states at both edges, and in one subphase the system exhibits no bound states while in the remaining two subphases the system exhibits a bound state at the left or the right edges.

Starting from the ground state, one can build up excitations in the bulk by adding spinons, strings, quartets [45], etc., and one obtains a tower of excited states. Similarly, starting from either the state which contains one bound state at the left or the right edge or from the state which contains two bound states, one can build up excitations in the bulk and one obtains different towers of excited states. Hence in the region where the system exhibits two bound states, the Hilbert space is comprised of four towers and in the regions where the system exhibits one bound state, the Hilbert space is comprised of two towers and in the regions where there exists no bound states, the Hilbert space is comprised of a single tower of excited states.

For a particular orientation of the boundary fields where the system exhibits a certain ground state, as the values of the magnetic fields is changed, the system undergoes a boundary eigenstate phase transition, where the system may gain or lose a bound state at a particular edge which results in the change in the number of towers in the Hilbert space. Across this phase transition line where the structure of the Hilbert space changes, the total spin S^z of the ground state of the system remains unchanged. To analyze the properties of the ground state across this phase transition, we chose the \mathbb{Z}_2 symmetric point where the values of the magnetic fields at the edges take equal values. By using DMRG we obtained the edge magnetization profile in the regions where the magnetic fields take values greater than and lesser than the critical field h_c . We find that when both the magnetic fields take values greater than the critical field, the total spin accumulation at each edge

saturates to $1/4$. To check whether this fractional spin is a genuine quantum observable, we calculated the variance and found that although it saturates to a small value, it remains nonzero, indicating that the fractional spin $1/4$ is not a genuine quantum number. Nevertheless, in the region where both the magnetic fields take values greater than the critical field, there exists nonzero probability to observe a nonzero spin S^z close to each edge. This suggests that one might observe a difference in the spin dynamics at the boundary across the phase transition line. Recently, such an effect was observed in the transverse field Ising model, where the dynamics of the spin at the edge depends on the number of edge states [48].

Although there exist no genuine spin fractionalization in the ground state, the structure of the Hilbert space and the boundary eigenstate phase transition the system exhibits are also found in the gapless superconductors which exhibit SPT. Even though the Hilbert space is comprised of towers of excited states, unlike the gapped regime of the XXZ spin-1/2 chain which exhibits SSB, degenerate pairing in the spectrum is not apparent due to the gapless nature of the bulk excitations. Although the model we considered is integrable, the structure of its Hilbert space and the boundary eigenstate phase transition it exhibits might provide insight into systems with disorder which exhibit phenomena such as many body localization.

ACKNOWLEDGMENTS

J.H.P. thanks W. Ketterle for useful discussions about realizing boundary fields in experiment. P.A. and P.R.P. thank F. H. L. Essler for very helpful discussions. J.L. and J.H.P. are partially supported by the Air Force Office of Scientific Research under Grant No. FA9550-20-1-0136 and the Alfred P. Sloan Foundation through a Sloan Research Fellowship. J.H.P. acknowledges the Aspen Center for Physics, where some of this work was discussed, which is supported by National Science Foundation Grant No. PHY-1607611. P.R.P. acknowledges support from Rutgers HEERF Fellowship during the stay at Rutgers University, where most part of the work was done.

APPENDIX A: SOLUTION OF BETHE ANSATZ EQUATIONS

In this section, we provide a detailed calculation of the ground state and the boundary excitations for chains with both odd and even numbers of sites chain in the phases A_1 , B_1 , and C_1 and describe how the solution in all the other phases can be constructed using the solution obtained in these phases.

1. A phases

Consider the phase A_1 . In this phase both the magnetic fields point in the positive z direction and take values $h_L, h_R > h_C$, ($h_C = 2$), which translates to the boundary parameters taking values $0 < p_L, p_R < 1/2$. The Bethe equations corresponding to Bethe reference state with all down spins are [2,28]

$$\left(\frac{\lambda_j - \frac{i}{2}}{\lambda_j + \frac{i}{2}}\right)^{2N} \left(\frac{\lambda_j + i(\frac{1}{2} + p_L)}{\lambda_j - i(\frac{1}{2} + p_L)}\right) \left(\frac{\lambda_j + i(\frac{1}{2} + p_R)}{\lambda_j - i(\frac{1}{2} + p_R)}\right) = \prod_{j \neq k=1}^{M-1} \left(\frac{\lambda_j - \lambda_k - i}{\lambda_j - \lambda_k + i}\right) \left(\frac{\lambda_j + \lambda_k - i}{\lambda_j + \lambda_k + i}\right). \quad (\text{A1})$$

The eigenvalues of the Hamiltonian are given by

$$E = - \sum_{j=1}^M \frac{2}{\lambda_j^2 + \frac{1}{4}} + N - 1 - \frac{1}{p_L} - \frac{1}{p_R}. \quad (\text{A2})$$

a. A_1 : odd number of sites

Let us first consider a state with all real Bethe roots. By applying logarithm to (A1), we obtain

$$(2N + 1)\Theta(2\lambda_j) - \Theta\left(\frac{\lambda_j}{\frac{1}{2} + p_L}\right) - \Theta\left(\frac{\lambda_j}{\frac{1}{2} + p_R}\right) = \sum_{\sigma=\pm} \sum_{k=1}^M \Theta(\lambda_j + \sigma\lambda_k) + \pi\nu(\lambda_j), \quad (\text{A3})$$

where $\Theta(x) = \arctan(x)$. We introduced the counting function $\nu(\lambda)$, where $\nu(\lambda_j) = I_j$. The constraint $j \neq k$ in the sum on the right side is lifted by introducing the term $\Theta(2\lambda_j)$ on the left side, which exactly cancels with the term corresponding to $\lambda_j = \lambda_k$ in the sum on the right side. Also note that due to the reflection symmetry of the Bethe equations (A1), if λ_k is a solution to the Bethe equations then $-\lambda_k$ is also a solution. To avoid the double counting, we associate both the roots $\lambda_j, -\lambda_j$ with the same integer I_j . Differentiating (A3) and noting that $\rho(\lambda) = \rho(-\lambda)$ and $2\rho(\lambda) = \frac{d}{d\lambda}\nu(\lambda)$, we obtain

$$(2N + 1)a_{\frac{1}{2}}(\lambda) - a_{\frac{1}{2}+p_L}(\lambda) - a_{\frac{1}{2}+p_R}(\lambda) = \pi\delta(\lambda) + 2\pi\rho_{|\frac{1}{2}\rangle}(\lambda) + 2\int_{-\infty}^{\infty} \rho_{|\frac{1}{2}\rangle}(\mu)a_1(\lambda - \mu)d\mu, \quad (\text{A4})$$

where $a_n(x) = \frac{n}{n^2+x^2}$. A hole at $\lambda = 0$ is added as $\lambda = 0$ is a trivial solution to the Bethe equations (A1) and leads to a zero wave function [28]. The reason for the subscripts for the density distribution will become evident soon.

Taking Fourier transform, we obtain

$$\tilde{\rho}_{|\frac{1}{2}\rangle}(\omega) = \frac{(2N + 1)e^{-\frac{|\omega|}{2}} - e^{-(\frac{1}{2}+p_L)|\omega|} - e^{-(\frac{1}{2}+p_R)|\omega|} - 1}{2(1 + e^{-|\omega|})}. \quad (\text{A5})$$

The total number of Bethe roots is $M_{|\frac{1}{2}\rangle} = \tilde{\rho}_{|\frac{1}{2}\rangle}(0) = \frac{N-1}{2}$, hence $S^z = -1/2$. We represent this state by $|\frac{1}{2}\rangle$. Notice that the number of roots is an integer only for a spin chain with odd number of sites.

Using (A2), one can find the energy of the states. Equation (A2) can be written as

$$E = -4\int_{-\infty}^{\infty} d\lambda a_{\frac{1}{2}}(\lambda)\rho(\lambda) + N - 1 - \frac{1}{p_L} - \frac{1}{p_R}. \quad (\text{A6})$$

Using the density distribution (A5) in the above equation, we obtain

$$E_{|\frac{1}{2}\rangle} = E_0 = -(2N + 1)\ln(4) + N - 1 + \pi + \sum_{i=L,R} \Psi\left(\frac{p_i}{2}\right) - \Psi\left(\frac{p_i - 1}{2}\right) - \frac{1}{p_i}, \quad (\text{A7})$$

where Ψ is the digamma function. There exists two boundary string solutions $\lambda_{p'_L} = \pm i(\frac{1}{2} + p_L)$, $\lambda_{p'_R} = \pm i(\frac{1}{2} + p_R)$ to the Bethe equations corresponding to all spin down Bethe reference state (A1). Adding $\lambda_{p'_L}$, we have

$$(2N + 1)a_{\frac{1}{2}}(\lambda) - a_{\frac{1}{2}+p_L}(\lambda) - a_{\frac{1}{2}+p_R}(\lambda) - a_{\frac{3}{2}+p_L}(\lambda) - a_{\frac{1}{2}-p_L}(\lambda) = \pi\delta(\lambda) + 2\pi\rho_{|0\rangle_{p'_L}}(\lambda) + 2\int_{-\infty}^{\infty} \rho_{|0\rangle_{p'_L}}(\mu)a_1(\lambda - \mu)d\mu.$$

Taking Fourier transform, we obtain

$$\tilde{\rho}_{|0\rangle_{p'_L}}(\omega) = \tilde{\rho}_{|\frac{1}{2}\rangle}(\omega) + \Delta\tilde{\rho}_{p'_L}(\omega), \quad \Delta\tilde{\rho}_{p'_L}(\omega) = -\frac{e^{(\frac{3}{2}+p_L)|\omega|} + e^{(\frac{1}{2}-p_L)|\omega|}}{2(1 + e^{-|\omega|})}. \quad (\text{A8})$$

The number of real roots is given by $M_{|0\rangle_{p'_L}} - 1 = \tilde{\rho}_{|0\rangle_{p'_L}}(0)$. From this, we obtain the total number of roots $M_{|0\rangle_{p'_L}} = N/2$, hence $S^z = 0$. We observe that the number of roots is an integer only if the number of sites is even. Since we have a chain with odd number of sites, in order for one to add a boundary string to the state $|\frac{1}{2}\rangle$, a propagating hole (spinon) needs to be added as well. Adding a spinon with rapidity θ , to the state $|\frac{1}{2}\rangle$ in addition to the boundary string $\lambda_{p'_L}$, we have

$$(2N + 1)a_{\frac{1}{2}}(\lambda) - a_{\frac{1}{2}+p_L}(\lambda) - a_{\frac{1}{2}+p_R}(\lambda) - a_{\frac{3}{2}+p_L}(\lambda) - a_{\frac{1}{2}-p_L}(\lambda) \quad (\text{A9})$$

$$= \pi\delta(\lambda) + \pi\delta(\lambda - \theta) + \pi\delta(\lambda + \theta) + 2\pi\rho_{|\frac{1}{2}\rangle_{(\theta,p'_L)}}(\lambda) + 2\int_{-\infty}^{\infty} \rho_{|\frac{1}{2}\rangle_{(\theta,p'_L)}}(\mu)a_1(\lambda - \mu)d\mu. \quad (\text{A10})$$

Taking Fourier transform, we obtain

$$\tilde{\rho}_{|\frac{1}{2}\rangle_{(\theta,p'_L)}}(\omega) = \tilde{\rho}_{|\frac{1}{2}\rangle}(\omega) + \Delta\tilde{\rho}_{p'_L}(\omega) + \Delta\tilde{\rho}_{\theta}(\omega), \quad \Delta\tilde{\rho}_{\theta}(\omega) = -\frac{\cos(\theta\omega)}{(1 + e^{-|\omega|})}. \quad (\text{A11})$$

The number of real roots is given by $M_{|0\rangle_{(\theta,p'_L)}} - 1 = \tilde{\rho}_{|0\rangle_{(\theta,p'_L)}}(0)$. From this, we find that the total number of Bethe roots is $M_{|\frac{1}{2}\rangle_{(\theta,p'_L)}} = \frac{N-1}{2}$, hence $S^z = -1/2$. We represent this state by $|\frac{1}{2}\rangle_{(\theta,L)}$. We can calculate the energy of this state using (A6),

we have

$$E_{|-\frac{1}{2}\rangle_{(\theta, p_L)}} = -4 \int_{-\infty}^{\infty} d\lambda a_{\frac{1}{2}}(\lambda) \rho_{|-\frac{1}{2}\rangle_{(\theta, L)}}(\lambda) + N - 1 - \frac{1}{p_L} - \frac{1}{p_R} - \frac{2}{\frac{1}{4} + (i(\frac{1}{2} + p_L))^2}. \quad (\text{A12})$$

Using (A14), in the above equation, we obtain

$$E_{|-\frac{1}{2}\rangle_{(\theta, L)}} = E_0 + \frac{2\pi}{\sin(\pi p_L)} + \frac{2\pi}{\cosh(\theta)}. \quad (\text{A13})$$

The first term is just the energy of the ground state $|-\frac{1}{2}\rangle$. The second term is the energy of the bound state at the left edge and the third term is the energy of the spinon with rapidity θ . The energy of both the spinon and the bound state are strictly positive with

$$0 < E_\theta < 2\pi, \quad E_{\text{bound state}} > 2\pi.$$

Similarly we can add the boundary string corresponding to the right boundary λ_{p_R} along with a spinon and obtain the state $|-\frac{1}{2}\rangle_{(\theta, R)}$ with total spin $S^z = -1/2$ described by the following density distribution

$$\tilde{\rho}_{|-\frac{1}{2}\rangle_{(\theta, p_R)}}(\omega) = \tilde{\rho}_{|-\frac{1}{2}\rangle}(\omega) + \Delta\tilde{\rho}_{p_R}(\omega) + \Delta\tilde{\rho}_\theta(\omega), \quad \Delta\tilde{\rho}_\theta(\omega) = -\frac{\cos(\theta\omega)}{(1 + e^{-|\omega|})} \quad (\text{A14})$$

with energy

$$E_{|-\frac{1}{2}\rangle_{(\theta, R)}} = E_0 + \frac{2\pi}{\sin(\pi p_R)} + \frac{2\pi}{\cosh(\theta)}. \quad (\text{A15})$$

Now consider the Bethe equations corresponding to all spin up reference state which can be obtained by taking $p_L \rightarrow -p_L$, $p_R \rightarrow -p_R$ [2] in Eqs. (A1) and (A2).

$$\left(\frac{\lambda_j - i/2}{\lambda_j + i/2}\right)^{2N} \left(\frac{\lambda_j + i(\frac{1}{2} - p_L)}{\lambda_j - i(\frac{1}{2} - p_L)}\right) \left(\frac{\lambda_j + i(\frac{1}{2} - p_R)}{\lambda_j - i(\frac{1}{2} - p_R)}\right) = \prod_{j \neq k=1}^{M-1} \left(\frac{\lambda_j - \lambda_k - i}{\lambda_j - \lambda_k + i}\right) \left(\frac{\lambda_j + \lambda_k - i}{\lambda_j + \lambda_k + i}\right).$$

The eigenvalues of the Hamiltonian are given by

$$E = -\sum_{j=1}^M \frac{2}{\lambda_j^2 + \frac{1}{4}} + N - 1 + \frac{1}{p_L} + \frac{1}{p_R}. \quad (\text{A16})$$

By applying logarithm and following the same procedure as above, we obtain the following distribution for the state with all real Bethe roots:

$$\tilde{\rho}_{|\frac{1}{2}\rangle}(\omega) = \frac{(2N + 1)e^{-\frac{|\omega|}{2}} - e^{-\left(\frac{1}{2} - p_L\right)|\omega} - e^{-\left(\frac{1}{2} - p_R\right)|\omega} - 1}{2(1 + e^{-|\omega|})}. \quad (\text{A17})$$

The total number of roots is given by $M_{|\frac{1}{2}\rangle} = \tilde{\rho}_{|\frac{1}{2}\rangle}(0)$. Using which we obtain $M_{|\frac{1}{2}\rangle} = \frac{N-1}{2}$. Using this we obtain $S^z = 1/2$. We represent this state by $|\frac{1}{2}\rangle$. By using (A16) and (A17), we obtain the following expression for the energy of the state $|\frac{1}{2}\rangle$:

$$E_{|\frac{1}{2}\rangle} = \frac{2\pi}{\sin(\pi p_L)} + \frac{2\pi}{\sin(\pi p_R)} + E_{|-\frac{1}{2}\rangle}. \quad (\text{A18})$$

Hence we find that this state contains bound states at the left and right edges, hence we represent this state by $|\frac{1}{2}\rangle_{L,R}$.

There exists states $|\frac{1}{2}\rangle_{(\theta, L)}$, $|\frac{1}{2}\rangle_{(\theta, R)}$ that are degenerate (in thermodynamic limit) to the states $|-\frac{1}{2}\rangle_{(\theta, L)}$, $|-\frac{1}{2}\rangle_{(\theta, R)}$ respectively obtained above. The state $|\frac{1}{2}\rangle_{(\theta, L)}$ contains a bound state at the left edge and a spinon. This state is obtained by adding the boundary string $\lambda_{p_R} = \pm i(\frac{1}{2} - p_R)$ which is a solution to (A16) and a spinon with rapidity θ . Following the same procedure as above, we obtain the following density distribution:

$$\tilde{\rho}_{|\frac{1}{2}\rangle_{(\theta, p_R)}}(\omega) = \tilde{\rho}_{|\frac{1}{2}\rangle}(\omega) + \Delta\tilde{\rho}_{p_R}(\omega) + \Delta\tilde{\rho}_\theta(\omega), \quad \Delta\tilde{\rho}_{p_R}(\omega) = -\frac{e^{\left(\frac{3}{2} - p_R\right)|\omega} + e^{\left(\frac{1}{2} + p_R\right)|\omega}}{2(1 + e^{-|\omega|})}. \quad (\text{A19})$$

The number of roots is given by $M_{|\frac{1}{2}\rangle_{(\theta, p_R)}} = \tilde{\rho}_{|\frac{1}{2}\rangle_{(\theta, p_R)}}(0)$. Using which we obtain $M_{|\frac{1}{2}\rangle_{(\theta, p_R)}} = \frac{N-1}{2}$. Using this, we obtain $S^z = 1/2$. The energy of this state can be obtained following the same procedure as above, we obtain

$$E_{|\frac{1}{2}\rangle_{(\theta, L)}} = E_{|\frac{1}{2}\rangle} - \frac{2\pi}{\sin(\pi p_R)} + \frac{2\pi}{\cosh(\theta)} \equiv E_{|-\frac{1}{2}\rangle} + \frac{2\pi}{\sin(\pi p_L)} + \frac{2\pi}{\cosh(\theta)}. \quad (\text{A20})$$

Hence it contains a bound state at the left edge and is degenerate with the state $|\frac{1}{2}\rangle_{(\theta,L)}$ obtained previously. We represent this state by $|\frac{1}{2}\rangle_{(\theta,L)}$. Similarly, by adding the boundary string $\lambda_{p_L} = \pm i(\frac{1}{2} - p_L)$ and a spinon to the state $|\frac{1}{2}\rangle$, we obtain the state $|\frac{1}{2}\rangle_{(\theta,R)}$.

Note that the bound state and the spinon both carry spin-1/2. When a bound state at either the left or the right edge is added to the state which has spin $S^z = -1/2$, the bound state's spin is oriented in the positive z direction. Now when a spinon is added its spin can be oriented along or opposite to that of the bound state, and hence the final resulting state $|\pm\frac{1}{2}\rangle_{(\theta,j)}$, where $j = L$ and R , has total spin $S^z = \pm 1/2$ depending on the spin orientation of the spinon.

From the above analysis, we see that for the odd chain, $|\frac{1}{2}\rangle$ is the ground state. One can add one bound state at either the left edge or the right edge accompanied by a spinon and one obtains the states $|\pm\frac{1}{2}\rangle_{(\theta,j)}$, where $j = L$ and R . One can also add two bound states one at each edge and one obtains the state $|\frac{1}{2}\rangle_{L,R}$. Starting from either of these six states, one can build up excitations in the bulk by adding even number of spinons and other type of Bethe roots such as 2-strings and quartets [44,45].

2. Summary of the results in the A_1 phase for a chain with the odd number of sites

Here we summarize the construction of the ground state and the excited states in the phase A_1 for odd number of sites. In the region A_1 , magnetic fields at both the boundaries point in the positive z direction.

Ground state. The ground state has total spin $S^z = -1/2$ with energy E_0 , exact expression of which is given by (A7) and is represented by $|\frac{1}{2}\rangle$. It contains $(N-1)/2$ all real Bethe roots and is constructed by starting with all spin down reference state.

Excitation with two boundary bound states. There exists a state $|\frac{1}{2}\rangle_{L,R}$ with total spin $S^z = 1/2$ which contains one exponentially localized spin $S^z = 1/2$ boundary bound state at each edge. It contains $(N-1)/2$ all real Bethe roots and is constructed by starting with reference state with all spin up. This state has energy $E_0 + m_R + m_L$, where $m_i = \frac{2\pi}{\sin(\pi p_i)}$ is the energy of the bound state.

Excitation with boundary bound state at the right edge. There exists a state with a bound state only at the right edge, represented by $|\frac{1}{2}\rangle_{(\theta,R)}$. It has total spin $S^z = -1/2$ and is obtained from the state $|\frac{1}{2}\rangle$ by adding imaginary Bethe root $\lambda_{p_R} = \pm i(\frac{1}{2} + p_R)$, which is called a boundary string. One also needs to add a spinon with rapidity θ in order to include the boundary string. There exists another state with a bound state at the right edge represented by $|\frac{1}{2}\rangle_{(\theta,R)}$. This state has total spin $S^z = 1/2$, and is obtained from the state $|\frac{1}{2}\rangle_{L,R}$ by adding the boundary string $\lambda_{p_L} = \pm i(\frac{1}{2} - p_L)$ and also a spinon with rapidity θ . The two states $|\frac{1}{2}\rangle_{(\theta,R)}$, $|\frac{1}{2}\rangle_{(\theta,R)}$ are degenerate in the thermodynamic limit and have energy $E_0 + E_\theta + E_R$ but differ in the spin orientation of the spinon which has spin $S^z = \pm 1/2$ respectively. Here $E_\theta = \frac{2\pi}{\cosh(\pi\theta)}$ is the energy of the spinon with rapidity θ .

Excitation with boundary bound state at the left edge. There exists two degenerate states with a bound state at the left edge represented by $|\pm\frac{1}{2}\rangle_{(\theta,L)}$, with energy $E_0 + m_L + E_\theta$. The state $|\frac{1}{2}\rangle_{(\theta,L)}$ has total spin $S^z = -1/2$ and can be obtained from the state $|\frac{1}{2}\rangle$ by adding the boundary string $\lambda_{p_L} = \pm i(\frac{1}{2} + p_L)$ and a spinon with rapidity θ , whose spin is $S^z = -1/2$. The state $|\frac{1}{2}\rangle_{(\theta,L)}$ has total spin $S^z = 1/2$ and is obtained from the state $|\frac{1}{2}\rangle$ by adding the boundary string $\lambda_{p_R} = \pm i(\frac{1}{2} - p_R)$ and a spinon with rapidity θ whose spin is $S^z = 1/2$.

a. A_1 : even number of sites

Now consider the spin chain with even number of sites. As seen in the previous section, starting with all spin down reference state and considering a state with all real roots one obtains the ground state $|\frac{1}{2}\rangle$. The number of roots in this state is $M = (N-1)/2$. N has to be odd in order for the number of roots to be an integer. To obtain the ground state for even number of sites, one needs to consider a state with one less Bethe root compared to the state $|\frac{1}{2}\rangle$, that is starting with all spin down reference state we need to include one spinon in addition to all real Bethe roots. Following the procedure described in the previous section, we obtain the following distribution:

$$\tilde{\rho}_{|\frac{1}{2}\rangle_\theta(\omega) = \frac{(2N+1)e^{-\frac{|\omega|}{2}} - e^{-\left(\frac{1}{2}+p_L\right)|\omega|} - e^{-\left(\frac{1}{2}+p_R\right)|\omega|} - 1}{2(1+e^{-|\omega|})} + \Delta\tilde{\rho}_\theta(\omega), \quad \Delta\tilde{\rho}_\theta(\omega) = -\frac{\cos(\theta\omega)}{(1+e^{-|\omega|})}. \quad (\text{A21})$$

The total number of Bethe roots is $M_{|\frac{1}{2}\rangle_\theta} = (N-2)/2$, hence $S^z = -1$. The number of roots is an integer only for a spin chain with even number of sites as desired. Note that the first term is same as the density distribution describing the state $|\frac{1}{2}\rangle$, with N now being even. The energy of this state can be calculated using (A2), we obtain

$$E_{|\frac{1}{2}\rangle_\theta} = E_0 + \frac{2\pi}{\cosh(\theta)}. \quad (\text{A22})$$

Hence in A_1 , the lowest energy state for even number of sites chain is parametrized by the rapidity of the spinon θ . The ground state is obtained in the limit where $\theta \rightarrow \infty$. Starting with all spin up reference state and considering a state with all real roots and a spinon we obtain

$$\tilde{\rho}_{|\frac{1}{2}\rangle_\theta(\omega) = \frac{(2N+1)e^{-\frac{|\omega|}{2}} - e^{-\left(\frac{1}{2}-p_L\right)|\omega|} - e^{-\left(\frac{1}{2}-p_R\right)|\omega|} - 1}{2(1+e^{-|\omega|})} + \Delta\tilde{\rho}_\theta(\omega). \quad (\text{A23})$$

The total number of Bethe roots is $M_{|1\rangle_\theta} = (N - 2)/2$, hence $S^z = 1$. The energy of this state can be calculated using (A16), we obtain

$$E_{|1\rangle_\theta} = E_0 + \frac{2\pi}{\sin(\pi p_L)} + \frac{2\pi}{\sin(\pi p_R)} + \frac{2\pi}{\cosh(\theta)}. \quad (\text{A24})$$

This state contains bound states at both the edges, and hence we represent this state by $|1\rangle_{(\theta,L,R)}$. Starting with all spin down reference state, consider a state with all real roots and the boundary string $\lambda_{p'_L} = \pm i(\frac{1}{2} + p_L)$. Following the similar procedure described in the previous section, we obtain

$$\tilde{\rho}_{|0\rangle_{p'_L}}(\omega) = \frac{(2N + 1)e^{-\frac{|\omega|}{2}} - e^{-\left(\frac{1}{2} + p_L\right)|\omega} - e^{-\left(\frac{1}{2} + p_R\right)|\omega} - 1}{2(1 + e^{-|\omega|})} + \Delta\tilde{\rho}_{p'_L}(\omega), \quad \Delta\tilde{\rho}_{p'_L}(\omega) = -\frac{e^{\left(\frac{3}{2} + p_L\right)|\omega} + e^{\left(\frac{1}{2} - p_L\right)|\omega}}{2(1 + e^{-|\omega|})}. \quad (\text{A25})$$

The total number of roots is $M_{|0\rangle_{p'_L}} = N/2$, and hence $S^z = 0$. We represent this state by $|0\rangle_L$. The energy of this state can be calculated using the procedure described in the previous section. We obtain

$$E_{|0\rangle_L} = E_0 + \frac{2\pi}{\sin(\pi p_L)}. \quad (\text{A26})$$

Similarly we can add the boundary string $\lambda_{p'_R} = \pm i(\frac{1}{2} + p_R)$ and obtain the state $|0\rangle_R$ which has energy $E_{|0\rangle_R} = E_0 + \frac{2\pi}{\sin(\pi p_R)}$. These states can also be obtained by starting with all spin up reference state, in which case, $|0\rangle_R$ and $|0\rangle_L$ contain all real roots and the boundary strings $\lambda_{p_L} = \pm i(\frac{1}{2} - p_L)$ and $\lambda_{p_R} = \pm i(\frac{1}{2} - p_R)$, respectively.

Starting with all spin down reference state, one can add both the boundary strings $\lambda_{p'_R}, \lambda_{p'_L}$ to the state with all real roots and one spinon. Following the regular procedure, we obtain the following density distribution

$$\tilde{\rho}_{|0\rangle_{(\theta p'_L, p'_R)}}(\omega) = \frac{(2N + 1)e^{-\frac{|\omega|}{2}} - e^{-\left(\frac{1}{2} + p_L\right)|\omega} - e^{-\left(\frac{1}{2} + p_R\right)|\omega} - 1}{2(1 + e^{-|\omega|})} + \Delta\tilde{\rho}_{p'_L}(\omega) + \Delta\tilde{\rho}_{p'_R}(\omega) + \Delta\tilde{\rho}_\theta(\omega). \quad (\text{A27})$$

The number of real roots is given by $M_{|0\rangle_{(\theta p'_L, p'_R)}} - 2 = \tilde{\rho}_{|0\rangle_{(\theta p'_L, p'_R)}}(0)$. From this we obtain that the total number of roots is $M_{|0\rangle_{(\theta p'_L, p'_R)}} = N/2$. This results in $S^z = 0$. We represent this state by $|0\rangle_{(\theta,L,R)}$. Calculating the energy we find that this state is degenerate with the state $|1\rangle_{(\theta,L,R)}$. Similarly, we can add both the boundary strings $\lambda_{p_R}, \lambda_{p_L}$ to the state $|1\rangle_\theta$ and obtain the state $|0\rangle_\theta$, which is degenerate with the state $|-1\rangle_\theta$.

3. Summary of the results in the A_1 phase for a chain with the even number of sites

Here we summarize the construction of the ground state and the excited states in the phase A_1 for even number of sites.

Ground state. In the phase A_1 , the ground state $|-1\rangle_\theta$ has total spin $S^z = -1$. It is constructed by starting with all spin down reference state and contains $(N - 2)/2$ real roots and a spinon with rapidity θ . In the thermodynamic limit, there exists another state $|0\rangle_\theta$ with total spin $S^z = 0$ which is degenerate with the ground state. This state is obtained by starting with all spin up reference state and in addition to $(N - 4)/2$ real roots it contains two boundary strings $\lambda_{p_R}, \lambda_{p_L}$ and a spinon with rapidity θ . The spin orientation of the spinon in the two ground states $|-1\rangle_\theta, |0\rangle_\theta$ is along the negative and positive z directions, respectively.

Excitation with a boundary bound state at the left edge. There exists a state represented by $|0\rangle_L$ which contains a bound state at the left edge and has total spin $S^z = 0$. This is constructed from the reference state with all spin down. In addition to $(N - 2)/2$ real roots, it contains one boundary string $\lambda_{p'_L}$ and has energy $E_0 + m_L$. This state can also be constructed from the reference state with all spin up and is made up of $(N - 2)/2$ real roots and one boundary string λ_{p_R} .

Excitation with a boundary bound state at the right edge. There exists a state $|0\rangle_R$ which contains a bound state at the right edge and has total spin $S^z = 0$. It is constructed from the reference state with all spin down and in addition to $(N - 2)/2$ real roots it contains one boundary string $\lambda_{p'_R}$ and has energy $E_0 + m_R$. This state can also be constructed from the reference state with all spin up and in addition to $(N - 2)/2$ real roots it contains one boundary string λ_{p_L} .

Excitation with two boundary bound states. There also exists a state $|0\rangle_{(\theta,L,R)}$ with total spin $S^z = 0$ which contains one bound state at each edge. It is constructed by starting with all spin down reference state and contains $(N - 4)/2$ real roots and two boundary strings $\lambda_{p'_L}, \lambda_{p'_R}$ and a spinon. The energy of the state is $E_0 + m_R + m_L + E_\theta$. In the thermodynamic limit, there exists another degenerate state $|1\rangle_{(\theta,L,R)}$ with total spin $S^z = 1$ that contains one bound state at each edge. This state is constructed by starting with all spin up reference state and contains $(N - 2)/2$ real roots and a spinon. The spin orientation of the spinon in the two states $|0\rangle_{(\theta,L,R)}$ and $|1\rangle_{(\theta,L,R)}$ is in the negative and positive z directions, respectively.

a. A_2 : odd number of sites

Construction of the states in the phase A_2 is similar to that in the A_1 phase, hence we skip the details of the calculation and provide an overview of how the ground state and boundary excited states are constructed in A_2 phase. The Bethe equations for all down and up reference states are obtained from (A1), (A2) and (A16), (A16) by making the transformation $p_L \rightarrow -p_L$.

Ground state. The ground state is twofold degenerate with energy $E_0 + E_\theta$ and is represented by $|\pm\frac{1}{2}\rangle_\theta$ with total spin $S^z = \pm 1/2$, respectively. $|\frac{1}{2}\rangle_\theta$ is constructed from all spin down reference state. It contains the boundary string λ_{p_L} and a

spinon in addition to $(N - 3)/2$ real roots. The state $|\frac{1}{2}\rangle_\theta$ is constructed by starting with all spin up reference state. It contains the boundary string λ_{p_R} and a spinon in addition to $(N - 3)/2$ real roots.

Excitation with a boundary bound state at the left edge. The state with a bound state at the left edge is represented by $|\frac{1}{2}\rangle_L$ and has total spin $S^z = -1/2$ and energy $E_0 + m_L$. It is constructed by starting with all spin down reference state and contains $(N - 1)/2$ all real roots.

Excitation with a boundary bound state at the right edge. The state with a bound state at the right edge is represented by $|\frac{1}{2}\rangle_R$ and has total spin $S^z = 1/2$ and energy $E_0 + m_R$. It is constructed by starting with all spin up reference state and contains $(N - 1)/2$ all real roots.

Excitation with two boundary bound states. The state with bound states at both the edges is twofold degenerate with energy $E_0 + m_L + m_R + E_\theta$ and is represented by $|\pm\frac{1}{2}\rangle_{(\theta,L,R)}$ with total spin $S^z = \pm 1/2$, respectively. $|\frac{1}{2}\rangle_{(\theta,L,R)}$ is constructed by starting with all spin up reference state and contains the boundary string $\lambda_{p'_L}$ and a spinon in addition to $(N - 3)/2$ real roots. $|\frac{1}{2}\rangle_{(\theta,L,R)}$ is constructed by starting with all spin down reference state and contains the boundary string $\lambda_{p'_R}$ and a spinon in addition to $(N - 3)/2$ real roots.

b. A_2 : even number of sites

Ground state. The ground state is represented by $|0\rangle$ and has energy E_0 and total spin $S^z = 0$. It is constructed by starting with all spin up reference state and contains the boundary string λ_{p_R} in addition to $(N - 2)/2$ real roots. It can also be constructed by starting with all spin down reference state and contains the boundary string $\lambda_{p'_L}$ in addition to $(N - 2)/2$ real roots.

Excitation with a boundary bound state at the left edge. The state which contains a bound state at the left edge is twofold degenerate with energy $E_0 + m_L + E_\theta$ and is represented by $|0\rangle_{(\theta,L)}$ and $|-1\rangle_{(\theta,L)}$ with total spin $S^z = 0$ and $S^z = -1$, respectively. The state $|0\rangle_{(\theta,L)}$ is constructed by starting with all spin up reference state. It contains the boundary strings $\lambda_{p_R}, \lambda_{p'_L}$ and a spinon in addition to $(N - 4)/2$ real roots. The state $|-1\rangle_{(\theta,L)}$ is constructed by starting with all spin down reference state and contains a spinon and $(N - 2)/2$ real roots.

Excitation with a boundary bound state at the right edge. The state which contains a bound state at the right edge is twofold degenerate with energy $E_0 + m_R + E_\theta$ and is represented by $|0\rangle_{(\theta,R)}$ and $|1\rangle_{(\theta,R)}$ with total spin $S^z = 0$ and $S^z = 1$ respectively. The state $|0\rangle_{(\theta,R)}$ is constructed by starting with all spin down reference state. It contains the boundary strings $\lambda_{p'_R}, \lambda_{p_L}$ and a spinon in addition to $(N - 4)/2$ real roots. The state $|1\rangle_{(\theta,R)}$ is constructed by starting with all spin up reference state and contains a spinon and $(N - 2)/2$ real roots.

Excitation with two boundary bound states. The state with bound states at both the edges is represented by $|0\rangle_{L,R}$ and has total spin $S^z = 0$ and energy $E_0 + m_L + m_R$. It is constructed by starting with all spin up reference state and contains the boundary string $\lambda_{p'_L}$ in addition to $(N - 2)/2$ real roots. It can also be constructed by starting with all spin down reference state and contains the boundary string $\lambda_{p'_R}$ in addition to $(N - 2)/2$ real roots.

c. Phase A_3 and A_4

In phases A_3 and A_4 , both the boundary magnetic fields point in the direction opposite that of phases A_1 and A_2 , respectively. Using the property (2), we can obtain all the states in phases A_3 and A_4 from the states obtained in phases A_1 and A_2 , respectively. In constructing a state in phase A_3 or A_4 , we can use the construction of the respective state in phase A_1 or A_2 , respectively, and use the following transformation:

$$|\uparrow\uparrow\dots\uparrow\rangle \leftrightarrow |\downarrow\downarrow\dots\downarrow\rangle, \quad p_L \rightarrow -p_L, \quad p_R \rightarrow p_R \quad (\text{A28})$$

where the all spin up and all spin down reference states are interchanged and the boundary magnetic fields change sign.

4. B phases

Consider phase B_1 . In this phase, both the magnetic fields point in the positive z direction and take the values $0 < h_R < h_C$ and $h_L > h_C$, which corresponds to the values $p_R > 1/2$ and $0 < p_L < 1/2$.

a. B_1 : odd number of sites

Consider the chain with odd number of sites. The Bethe equations corresponding to all spin down reference state are given by (A1). The eigenvalues of the Hamiltonian are given by (A2). The ground state contains all real roots and we obtain the distribution (A5) with energy E_0 and spin $S^z = -1/2$. Now by adding the boundary string $\lambda_{p'_L}$ along with a spinon, we obtain the state $|\frac{1}{2}\rangle_{(\theta,L)}$ which contains a bound state at the left edge. This state has total spin $S^z = -1/2$ and energy $E_0 + m_L + E_\theta$.

Now consider all spin up reference state. The eigenvalues are given by (A16) where as the Bethe equations (A16) take the form

$$\left(\frac{\lambda_j - i/2}{\lambda_j + i/2}\right)^{2N} \left(\frac{\lambda_j + i(\frac{1}{2} - p_L)}{\lambda_j - i(\frac{1}{2} - p_L)}\right) \left(\frac{\lambda_j - i(p_R - \frac{1}{2})}{\lambda_j + i(p_R - \frac{1}{2})}\right) = \prod_{j \neq k=1}^{M-1} \left(\frac{\lambda_j - \lambda_k - i}{\lambda_j - \lambda_k + i}\right) \left(\frac{\lambda_j + \lambda_k - i}{\lambda_j + \lambda_k + i}\right).$$

Considering the state with all real roots and following the same procedure as in the previous section, we obtain

$$\tilde{\rho}_{|0\rangle}(\omega) = \frac{(2N+1)e^{-\frac{|\omega|}{2}} - e^{-\left(\frac{1}{2}-p_L\right)|\omega|} + e^{-\left(p_R-\frac{1}{2}\right)|\omega|} - 1}{2(1+e^{-|\omega|})}. \quad (\text{A29})$$

The total number of roots given by $M = \tilde{\rho}_{|0\rangle}(0) = N/2$. Hence we find that the number of roots is not an integer for odd number of sites. Hence we need to consider the state with one spinon along with real roots. We obtain

$$\tilde{\rho}_{|\frac{1}{2}\rangle_{\theta}}(\omega) = \frac{(2N+1)e^{-\frac{|\omega|}{2}} - e^{-\left(\frac{1}{2}-p_L\right)|\omega|} + e^{-\left(p_R-\frac{1}{2}\right)|\omega|} - 1}{2(1+e^{-|\omega|})} + \Delta\tilde{\rho}_{\theta}(\omega). \quad (\text{A30})$$

The number of roots is given by $M = \tilde{\rho}_{|\frac{1}{2}\rangle_{\theta}}(0) = (N-1)/2$, and hence the number of roots is an integer for odd number of sites and we obtain $S^z = 1/2$. The energy of this state can be calculated using (A16). Following the procedure described in the previous section, we obtain $E_{|\frac{1}{2}\rangle_{\theta}} = E_0 + m_L + E_{\theta}$. Hence this state contains a bound state at the left edge and is degenerate with the state $|-\frac{1}{2}\rangle_{(\theta,L)}$ obtained above. We represent this state by $|\frac{1}{2}\rangle_{(\theta,L)}$.

5. Summary of the results in the B_1 phase for a chain with the odd number of sites

Ground state. The ground state has total spin $S^z = -1/2$ and is represented by $|-\frac{1}{2}\rangle$. This state is constructed by starting with all spin down reference state and contains $(N-1)/2$ real roots and has energy E_0 .

Excitation with bound state at the left edge. There exists a state which contains a bound state at the left edge, which is represented by $|-\frac{1}{2}\rangle_{(\theta,L)}$ and has total spin $S^z = -1/2$ and energy $E_0 + E_{\theta} + m_L$. This state is obtained from the state $|-\frac{1}{2}\rangle$ by adding the boundary string λ_{p_L} and a spinon with rapidity θ . There exists a degenerate state $|\frac{1}{2}\rangle_{(\theta,L)}$ which contains a bound state at the left edge and has total spin $S^z = 1/2$. This state is obtained by starting with reference state with all spin up. It contains $(N-1)/2$ real roots and a spinon with rapidity θ .

a. B_1 : even number of sites

Now consider the chain with even number of sites. The Bethe equation corresponding to all spin up reference state have the boundary string solution λ_{p_L} . Consider a state with this boundary string and a spinon in addition to real roots. By following the usual procedure, we obtain the following distribution:

$$\tilde{\rho}_{|0\rangle_{(\theta,p_L)}}(\omega) = \frac{(2N+1)e^{-\frac{|\omega|}{2}} - e^{-\left(\frac{1}{2}-p_L\right)|\omega|} + e^{-\left(p_R-\frac{1}{2}\right)|\omega|} - 1}{2(1+e^{-|\omega|})} + \Delta\tilde{\rho}_{p_L}(\omega) + \Delta\tilde{\rho}_{\theta}(\omega). \quad (\text{A31})$$

The number of real roots is given by $M_{|0\rangle_{(\theta,p_L)}} - 1 = \tilde{\rho}_{|0\rangle_{(\theta,p_L)}}(0) = (N-2)/2$, hence we obtain that the total number of roots is $M_{|0\rangle_{(\theta,p_L)}} = N/2$ and hence $S^z = 0$. The energy can be calculated using (A16), we obtain $E_{|0\rangle_{(\theta,p_L)}} = E_0 + E_{\theta}$. Starting with the spin down reference state, consider the state with one spinon in addition to real roots. We obtain the following distribution:

$$\tilde{\rho}_{|-1\rangle_{\theta}}(\omega) = \frac{(2N+1)e^{-\frac{|\omega|}{2}} - e^{-\left(\frac{1}{2}-p_L\right)|\omega|} - e^{-\left(\frac{1}{2}-p_R\right)|\omega|} - 1}{2(1+e^{-|\omega|})} + \Delta\tilde{\rho}_{\theta}(\omega). \quad (\text{A32})$$

The number of roots is given by $M_{|-1\rangle_{\theta}} = (N-2)/2$, hence $S^z = -1$. The energy of this state can be calculated using (A2), and we obtain $E_{|-1\rangle_{\theta}} = E_0 + E_{\theta}$. Hence the ground state is twofold degenerate with energy $E_0 + E_{\theta}$. It is represented by $|0\rangle_{\theta}$ and $|-1\rangle_{\theta}$ with total spin $S^z = 0$ and -1 , respectively.

Starting with all spin up reference state, consider the state with all real roots. We obtain the following distribution:

$$\tilde{\rho}_{|0\rangle}(\omega) = \frac{(2N+1)e^{-\frac{|\omega|}{2}} - e^{-\left(\frac{1}{2}-p_L\right)|\omega|} + e^{-\left(p_R-\frac{1}{2}\right)|\omega|} - 1}{2(1+e^{-|\omega|})}. \quad (\text{A33})$$

The number of roots is given by $M_{|0\rangle} = \tilde{\rho}_{|0\rangle}(0) = N/2$, and hence it has total spin $S^z = 0$. The energy of this state can be calculated using (A16), we obtain $E_{|0\rangle} = E_0 + m_L$. Hence it has a bound state at the left edge. This state is represented by $|0\rangle_L$.

6. Summary of the results in the B_1 phase for a chain with the even number of sites

Ground state. The ground state is twofold degenerate. The ground state $|-1\rangle_{\theta}$, with total spin $S^z = -1$ is constructed by starting with all spin down reference state and contains $(N-2)/2$ real roots and a spinon with rapidity θ . The ground state $|0\rangle_{\theta}$ with total spin $S^z = 0$ is constructed by starting with all spin up reference state. It contains a spinon and the boundary string λ_{p_L} in addition to $(N-2)/2$ real roots. The spin orientation of the spinon in the states $|-1\rangle_{\theta}$ and $|0\rangle_{\theta}$ is along the negative and positive z directions, respectively.

Excitation with a boundary bound state at the left edge. There exists a state $|0\rangle_L$ with a bound state at the left boundary. It has total spin $S^z = 0$ and is constructed by starting with all spin up reference state and contains $N/2$ real roots. It can also be

constructed by starting with all spin down reference state and it includes the boundary string λ_{p_L} in addition to $(N - 2)/2$ real roots.

a. Phase B_2 : odd number of sites chain

The construction of the state in phase B_2 is similar to that in phase B_1 , hence we skip the details of the calculation and provide an overview of how the ground state and boundary excited states are constructed in phase B_2 .

Ground state. The ground state is twofold degenerate with energy $E_0 + E_\theta$. It is represented by $|\pm\frac{1}{2}\rangle_\theta$ with total spin $S^z = \pm 1/2$. The state $|\frac{1}{2}\rangle_\theta$ is obtained by starting with reference state with all spin up and it contains a spinon in addition to $(N - 2)/2$ real Bethe roots. The state $|\frac{1}{2}\rangle_\theta$ is obtained by starting with all spin down reference state and contains the boundary string λ_{p_L} and a spinon in addition to real roots.

Excitation with a boundary bound state at the left edge. The state with the bound state at the left edge has energy $E_0 + m_L$ and total spin $S^z = -1/2$. It is represented by $|\frac{1}{2}\rangle_L$ and is constructed by starting with all spin down reference state and contains all real roots.

b. Phase B_2 : even number of sites chain

Ground state. The ground state $|0\rangle$ has energy E_0 and total spin $S^z = 0$. It is obtained by starting with reference state with all spin up and it contains $N/2$ all real roots. It can also be obtained by starting with all spin down reference state and it contains the boundary string λ_{p_L} in addition to $(N - 2)/2$ real roots.

Excitation with a boundary bound state at the left edge. The state with the bound state at the left edge is doubly degenerate with energy $E_0 + m_L + E_\theta$ and is represented by $|-1\rangle_{(\theta,L)}$ and $|0\rangle_{(\theta,L)}$ with total spin $S^z = -1$ and 0 , respectively. The state $|-1\rangle_{(\theta,L)}$ is obtained by starting with all spin down reference state and contains one spinon in addition to $(N - 2)/2$ real roots. The state $|0\rangle_{(\theta,L)}$ is obtained by starting with all spin all reference state. It contains the boundary string λ_{p_L} and a spinon in addition to $(N - 2)/2$ real roots.

c. Other B phases

The states in phases B_8 and B_7 can be obtained from the states in phases B_1 and B_2 respectively by the transformation $p_L \leftrightarrow p_R$. The states in phases B_5 , B_6 , B_3 , and B_4 can be obtained from the states in phases B_1 , B_2 , B_7 , and B_8 respectively by the transformation (A28).

7. C phases

a. Odd number of sites

In subregion C_1 , the ground state is $|\frac{1}{2}\rangle$ with total spin $S^z = -1/2$. This state is constructed from the reference state with all down spins and contains $(N - 1)/2$ real roots. In C_3 , the ground state is $|\frac{1}{2}\rangle$ with total spin $S^z = 1/2$. This state is constructed from the reference state with all up spins and contains $(N - 1)/2$ real roots. In subregions C_2 and C_4 , the ground state is twofold degenerate and contains a spinon with rapidity θ . The spin orientation of the spinon dictates the total spin $S^z = \pm 1/2$ of the state. They are represented by $|\pm\frac{1}{2}\rangle_{(\pm,\theta)}$, and contain $(N - 1)/2$ real roots and a spinon with rapidity θ , and constructed from either all spin up or down reference states and contain all real roots and a spinon with rapidity θ .

b. Even number of sites

In subregion C_I , the ground state is twofold degenerate in thermodynamic limit and is represented by $|0\rangle_\theta$, $|-1\rangle_\theta$ with total spin $S^z = 0$ and -1 , respectively. The state $|0\rangle_\theta$ is constructed from the reference state with all up spin and contains $N/2$ real roots and a spinon with rapidity θ . the state $|-1\rangle_\theta$ is constructed with the reference state with all down spins and contains $(N - 2)/2$ real roots and a spinon with rapidity θ . The spin orientation of the spinon is in the negative and positive z directions in the states $|-1\rangle_\theta$ and $|0\rangle_\theta$, respectively. In subregion C_3 , the ground state is twofold degenerate and is represented by $|0\rangle_\theta$, $|1\rangle_\theta$ with total spin $S^z = 0$ and 1 , respectively. $|0\rangle_\theta$ contains a spinon with rapidity θ , the spin orientation of which is in the negative z direction. It is constructed from the reference state with all spin down and contains $N/2$ real roots and a spinon with rapidity θ . $|1\rangle_\theta$ is constructed with the reference state with all spin up and contains $(N - 2)/2$ real roots and a spinon with rapidity θ with spin oriented in the positive z direction. In subregions C_2 and C_4 , the ground state has total spin $S^z = 0$ and is represented by $|0\rangle$. It can be constructed from the reference state with all spin up or all spin down and contains $N/2$ real roots.

APPENDIX B: BOUND STATE WAVE FUNCTION

In this section, we provide the bound state wave function corresponding to the boundary string in one particle sector (one flipped spin). Let us consider the subphase A_1 . The Bethe equations corresponding to all spin down reference state in one particle sector are given by

$$\left(\frac{\lambda - \frac{i}{2}}{\lambda + \frac{i}{2}}\right)^{2N} \left(\frac{\lambda + i(\frac{1}{2} + p_L)}{\lambda - i(\frac{1}{2} + p_L)}\right) \left(\frac{\lambda + i(\frac{1}{2} + p_R)}{\lambda - i(\frac{1}{2} + p_R)}\right) = 1. \quad (\text{B1})$$

The wave function is given by [30,31]

$$f(x) = \left(\frac{\lambda + \frac{i}{2}}{\lambda - \frac{i}{2}} \right)^{N-x} \left(\frac{\lambda - i(\frac{1}{2} + p_R)}{p_R(\lambda - \frac{i}{2})} \right) - \left(\frac{\lambda - \frac{i}{2}}{\lambda + \frac{i}{2}} \right)^{N-x} \left(\frac{\lambda + i(\frac{1}{2} + p_R)}{p_R(\lambda + \frac{i}{2})} \right). \quad (\text{B2})$$

When $\lambda = \pm i(\frac{1}{2} + p_R)$, which is the boundary string associated with the right edge, we readily obtain the wave function for the bound state localized at the right edge

$$f_R(x) = \pm \left(\frac{1 + 2p_R}{p_R(1 + p_R)} \right) \left(\frac{1 + p_R}{p_R} \right)^{-(N-x)}. \quad (\text{B3})$$

To obtain the bound state wave function associated with the left edge, we multiply the wave function (B2) with a normalization constant

$$\mathcal{A} = \left(\frac{p_R}{p_L} \right) \left(\frac{\lambda + i(\frac{1}{2} + p_L)}{\lambda + i(\frac{1}{2} + p_R)} \right) \left(\frac{\lambda - i(\frac{1}{2} + p_L)}{\lambda - i(\frac{1}{2} + p_R)} \right) \quad (\text{B4})$$

and use the one particle Bethe equation (B1). We obtain

$$\mathcal{A}f(x) = \left(\frac{\lambda + \frac{i}{2}}{\lambda - \frac{i}{2}} \right)^{-x} \left(\frac{\lambda + i(\frac{1}{2} + p_L)}{p_L(\lambda - \frac{i}{2})} \right) - \left(\frac{\lambda - \frac{i}{2}}{\lambda + \frac{i}{2}} \right)^{-x} \left(\frac{\lambda - i(\frac{1}{2} + p_L)}{p_L(\lambda + \frac{i}{2})} \right). \quad (\text{B5})$$

When $\lambda = \pm i(\frac{1}{2} + p_L)$, which is the boundary string associated with the left edge, we obtain the bound state wave function localized at the left edge

$$f_L(x) = \pm \left(\frac{1 + 2p_L}{p_L^2} \right) \left(\frac{1 + p_L}{p_L} \right)^{-x}. \quad (\text{B6})$$

Hence, we find that the two boundary string solutions correspond to exponentially localized bound states $\sim e^{-\kappa_L x}$ and $\sim e^{-\kappa_R(N-x)}$, where

$$\kappa_j = \ln(h_j + 1), \quad j = L \text{ and } R. \quad (\text{B7})$$

Note that when the magnetic fields at the edges take equal values $h_L = h_R = h$ ($p_L = p_R = p$), the normalization constant $\mathcal{A} = 1$. To obtain the bound state wave functions in this case, consider

$$f(x) \pm \left(\frac{p}{1+p} \right) f(x). \quad (\text{B8})$$

In this limit, we only have one boundary string solution $\lambda = \pm i(\frac{1}{2} + p)$, corresponding to the double pole of the Bethe equations (B1). Using this in (B8), we obtain

$$f(x)_{\pm} = - \left(\frac{1 + 2p}{p(1+p)} \right) \left[\left(\frac{1+p}{p} \right)^{-(N-x)} \pm \left(\frac{1+p}{p} \right)^{-x} \right] \quad (\text{B9})$$

Hence, we find that when $h_L = h_R$, in contrast to [31], there exist two bound states solutions simultaneously localized at both the edges

$$f(x)_{\pm} \sim (e^{-\kappa(N-x)} \pm e^{-\kappa x}), \quad \kappa = \ln(h + 1). \quad (\text{B10})$$

APPENDIX C: DETAILS AND VALIDITY OF THE FITTING

In Figs. 7(b) and 8(c), we have indicated the region where the fitting to Eq. (47) numerically fails with a shade. Here, we show that this is merely due to numerical overfittings and is not of physical consequence.

First, we interpolate the data in Fig. 7(b) through the missing region. Some data points in the figure near $h_c = 2$ are additionally excluded in the interpolation to make the interpolated function smooth. The results, together with the original Fig. 7(b), are plotted in Fig. 11(a). Now we take the values from the interpolated function for C and D and refit to Eq. (47) to obtain A and B . This results are shown in Figs. 11(b) and 8(b) in the main text. For the special point $h = 2$, $C = D = 0$ is used in the fit, and note that the resulting A and B fit parameters are smooth near $h = 2$. The A, B data away from $h = 2$ in Fig. 11(b) are identical to that obtained from the calculation in Figs. 7(b) and 8(c).

Finally, we use the newly fitted parameters A to D from Figs. 11(a) and 11(b) and compare with the original $S^z(x_i)$ data for the shaded region, which are $h = 1.90, 1.95, 2.05$, in Fig. 11(c). [$h = 2.00$ data are included in Fig. 7(a).] The agreement between the data and fit is excellent in all three values of h . This demonstrates that the fitting failure at the shaded region is because of overfitting, and the true physics in those parameters connect smoothly to the behavior outside the region. We also claim that

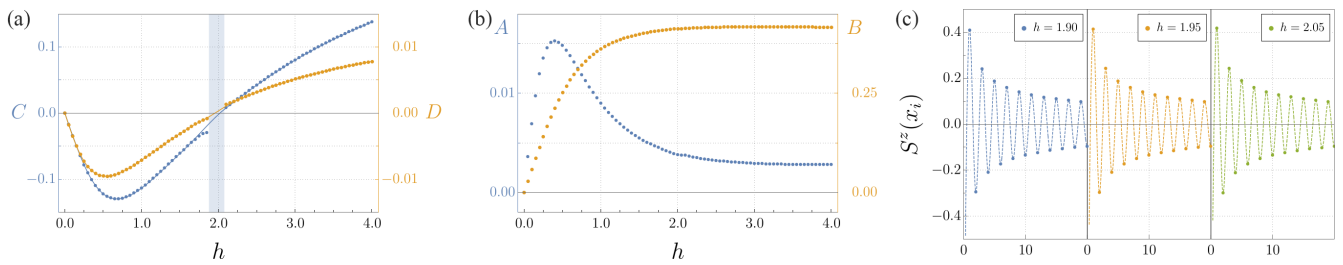


FIG. 11. (a) The same figure from Fig. 7(b) together with the smooth interpolating function through the missing region. (b) Fitting parameters A and B [see Eq. (47)] with the substitution of C and D with the interpolated function obtained in (a). (c) Magnetization data (dots) and its fit to Eq. (47) (dashed lines) of the h values of the shaded region using the parameters obtained in (a), (b) for the first 20 sites of the $N = 1000$ chain. The good agreement between the data and fit demonstrates the interpolation in (a) is valid.

small deviations from the interpolated function and data (for example, C near $h = 1.8$) are also the result of such numerical issues of overfit, while less serious than that more closer to $h = 2$.

-
- [1] H. Bethe, *Z. Phys.* **71**, 205 (1931).
 [2] E. K. Sklyanin, *J. Phys. A: Math. Gen.* **21**, 2375 (1988).
 [3] C. N. Yang and C. P. Yang, *Phys. Rev.* **150**, 321 (1966).
 [4] A. Pal and D. A. Huse, *Phys. Rev. B* **82**, 174411 (2010).
 [5] D. A. Abanin, E. Altman, I. Bloch, and M. Serbyn, *Rev. Mod. Phys.* **91**, 021001 (2019).
 [6] E. Ilievski, J. De Nardis, M. Medenjak, and T. C. V. Prosen, *Phys. Rev. Lett.* **121**, 230602 (2018).
 [7] E. Ilievski, J. De Nardis, B. Wouters, J.-S. Caux, F. H. L. Essler, and T. Prosen, *Phys. Rev. Lett.* **115**, 157201 (2015).
 [8] M. Dupont and J. E. Moore, *Phys. Rev. B* **101**, 121106(R) (2020).
 [9] M. Steiner, J. Villain, and C. Windsor, *Adv. Phys.* **25**, 87 (1976).
 [10] S. K. Satija, J. D. Axe, G. Shirane, H. Yoshizawa, and K. Hirakawa, *Phys. Rev. B* **21**, 2001 (1980).
 [11] S. E. Nagler, D. A. Tennant, R. A. Cowley, T. G. Perring, and S. K. Satija, *Phys. Rev. B* **44**, 12361 (1991).
 [12] D. A. Tennant, R. A. Cowley, S. E. Nagler, and A. M. Tsvetlik, *Phys. Rev. B* **52**, 13368 (1995).
 [13] J.-M. Maillet, *Prog. Math. Phys.* **53**, 161 (2007).
 [14] P. N. Jepsen, W. W. Ho, J. Amato-Grill, I. Dimitrova, E. Demler, and W. Ketterle, *Phys. Rev. X* **11**, 041054 (2021).
 [15] P. N. Jepsen, Y. K. Lee, H. Lin, I. Dimitrova, Y. Margalit, W. W. Ho, and W. Ketterle, *Nat. Phys.* **18**, 899 (2022).
 [16] C. N. Yang and C. P. Yang, *Phys. Rev.* **150**, 327 (1966).
 [17] C. N. Yang and C. P. Yang, *Phys. Rev.* **151**, 258 (1966).
 [18] O. Babelon, H. de Vega, and C. Viallet, *Nucl. Phys. B* **220**, 13 (1983).
 [19] H. E. Boos and V. E. Korepin, *J. Phys. A: Math. Gen.* **34**, 5311 (2001).
 [20] N. Kitanine, J. Maillet, and V. Terras, *Nucl. Phys. B* **567**, 554 (2000).
 [21] M. Shiroishi and M. Takahashi, *J. Phys. Soc. Jpn.* **74**, 47 (2005).
 [22] M. Takahashi, *Thermodynamics of One-Dimensional Solvable Models* (Cambridge University Press, Tokyo, 1999).
 [23] I. V. Cherednik, *Theor. Math. Phys.* **61**, 977 (1984).
 [24] M. T. Grisaru, L. Mezincescu, and R. I. Nepomechie, *J. Phys. A: Math. Gen.* **28**, 1027 (1995).
 [25] J. Cao, H.-Q. Lin, K.-J. Shi, and Y. Wang, [arXiv:cond-mat/0212163](https://arxiv.org/abs/cond-mat/0212163).
 [26] Y. Qiao, J. Cao, W.-L. Yang, K. Shi, and Y. Wang, *Phys. Rev. B* **103**, L220401 (2021).
 [27] P. Sun, Z.-R. Xin, Y. Qiao, K. Hao, L. Cao, J. Cao, T. Yang, and W.-L. Yang, *J. Phys. A: Math. Theor.* **52**, 265201 (2019).
 [28] Y. Wang, W.-L. Yang, J. Cao, and K. Shi, *Off-Diagonal Bethe Ansatz for Exactly Solvable Models* (Springer, Berlin, 2015).
 [29] Y. Wang, *Phys. Rev. B* **56**, 14045 (1997).
 [30] F. C. Alcaraz, M. N. Barber, M. T. Batchelor, R. J. Baxter, and G. R. W. Quispel, *J. Phys. A: Math. Gen.* **20**, 6397 (1987).
 [31] S. Skorik and H. Saleur, *J. Phys. A: Math. Gen.* **28**, 6605 (1995).
 [32] A. Kapustin and S. Skorik, *J. Phys. A: Math. Gen.* **29**, 1629 (1996).
 [33] S. Grijalva, J. Nardis, and V. Terras, *SciPost Phys.* **7**, 023 (2019).
 [34] All our Bethe ansatz results are in the thermodynamic limit. In this limit, even though the number of sites is very large, the ground state spin depends on whether the number of sites is even or odd.
 [35] A. Keselman and E. Berg, *Phys. Rev. B* **91**, 235309 (2015).
 [36] A. Keselman, E. Berg, and P. Azaria, *Phys. Rev. B* **98**, 214501 (2018).
 [37] P. R. Pasnoori, N. Andrei, and P. Azaria, *Phys. Rev. B* **102**, 214511 (2020).
 [38] P. R. Pasnoori, N. Andrei, and P. Azaria, *Phys. Rev. B* **104**, 134519 (2021).
 [39] P. Fendley, *J. Phys. A: Math. Theor.* **49**, 30LT01 (2016).
 [40] I. Affleck and E. H. Lieb, *Lett. Math. Phys.* **12**, 57 (1986).
 [41] H. Tasaki, *Physics and Mathematics of Quantum Many-Body Systems* (Springer Cham, Switzerland, 2020).
 [42] In the finite system, the size limit for the chains with the odd number of sites, the ground states in the second and the fourth quadrants are exactly degenerate on the line in the phase diagram corresponding to $|h_l| = |h_r|$. away from this line, the ground states are quasidegenerate and the true ground state corresponds to the spin orientation of the spinon pointing in the

- direction opposite to the boundary field which has the highest magnitude.
- [43] In the finite system, the size limit for the chains with the even number of sites, the ground states in the first and third quadrants are only quasidegenerate, where in the true ground state, the spinon's spin points in the opposite direction to the boundary magnetic fields.
- [44] C. Destri and J. H. Lowenstein, *Nucl. Phys. B* **205**, 369 (1982).
- [45] When a boundary string corresponding to a particular edge is added, new higher order boundary string solutions appear [31]. these higher order boundary strings can only be added in the presence of spinons and they describe certain excited states. note that a state with a boundary string or a set of boundary strings may not necessarily contain a bound state.
- [46] M. Fishman, S. R. White, and E. M. Stoudenmire, *SciPost Phys. Codebases* **4** (2022).
- [47] R. Jackiw, A. Kerman, I. Klebanov, and G. Semenoff, *Nucl. Phys. B* **225**, 233 (1983).
- [48] U. Javed, J. Marino, V. Oganessian, and M. Kolodrubetz, Counting edge modes via dynamics of boundary spin impurities (unpublished).